

CTCF promotes colorectal cancer cell proliferation and chemotherapy resistance to 5-FU via the P53-Hedgehog axis

Qihua Lai^{1,*}, Qingyuan Li^{1,*}, Chengcheng He¹, Yuxin Fang¹, Simin Lin¹, Jianqun Cai¹, Jian Ding¹, Qian Zhong¹, Yue Zhang¹, Changjie Wu¹, Xinke Wang¹, Juan He¹, Yongfeng Liu¹, Qun Yan¹, Aimin Li^{1,&}, Side Liu^{1,&}

¹Guangdong Provincial Key Laboratory of Gastroenterology, Department of Gastroenterology, Nanfang Hospital, Southern Medical University, Guangzhou, Guangdong, China

*Equal contribution

Correspondence to: Side Liu, Aimin Li; email: liuside2011@163.com, lam0725@qq.com

Keywords: colorectal cancer, CTCF, Hedgehog, P53, chemotherapy resistance

Received: March 7, 2020

Accepted: June 19, 2020

Published: July 20, 2020

Copyright: Lai et al. This is an open-access article distributed under the terms of the Creative Commons Attribution License (CC BY 3.0), which permits unrestricted use, distribution, and reproduction in any medium, provided the original author and source are credited.

ABSTRACT

CTCF is overexpressed in several cancers and plays crucial roles in regulating aggressiveness, but little is known about whether CTCF drives colorectal cancer progression. Here, we identified a tumor-promoting role for CTCF in colorectal cancer. Our study demonstrated that CTCF was upregulated in colorectal cancer specimens compared with adjacent noncancerous colorectal tissues. The overexpression of CTCF promoted colorectal cancer cell proliferation and tumor growth, while the opposite effects were observed in CTCF knockdown cells. Increased GLI1, Shh, PTCH1, and PTCH2 levels were observed in CTCF-overexpressing cells using western blot analyses. CCK-8 and apoptosis assays revealed that 5-fluorouracil chemosensitivity was negatively associated with CTCF expression. Furthermore, we identified that P53 is a direct transcriptional target gene of CTCF in colorectal cancer. Western blot and nuclear extract assays showed that inhibition of P53 can counteract Hedgehog signaling pathway repression induced by CTCF knockdown. In conclusion, we uncovered a crucial role for CTCF regulation that possibly involves the P53-Hedgehog axis and highlighted the clinical utility of colorectal cancer-specific potential therapeutic target as disease progression or clinical response biomarkers.

INTRODUCTION

Colorectal cancer (CRC) is the third most malignant cancer worldwide and one of the most common tumors of the digestive tract, causing over 600 000 deaths annually [1–4]. Although progress has been made in the development of therapies, including various surgical methods, chemotherapy, radiotherapy and immunotherapy, the prognosis of CRC patients remains unsatisfactory; increasing rates of chemoradiotherapy resistance, local recurrence and distant metastasis result in a poor prognosis among CRC patients [5–9]. A large number of studies have shown that dysregulated genes and the abnormal activation or inhibition of tumor-associated signaling pathways are involved in the initiation and progression of CRC [10–12]. Therefore,

we need to gain a more comprehensive understanding of the molecular mechanism involved in the development and progression of CRC and to develop more specific screening tests for the early detection and identification of colorectal tumors with a greater risk of progression.

CTCC-binding factor (CTCF), a transcription factor with 11 zinc fingers (ZFs), is highly conserved despite being over 700 amino acids long [13]. Many intensive studies have reported that CTCF functions as a versatile nuclear factor involved in transcriptional inhibition or activation [14–16], insulation [17, 18], silencers or enhancers [13, 18], gene imprinting [19, 20], controlling X chromosome inactivation in females [21], etc. Most CTCF functions are linked to its ability to regulate three-dimensional (3D) chromatin structure by forming sequence-specific

DNA loops [13, 19]. As a multifunctional transcription factor, CTCF was reported to be involved in the initiation of multiple cancers, including breast cancer [18], hepatocellular carcinoma [22], lung cancer [14], prostate cancer [23], etc., which could be attributed to the abnormal expression of CTCF or the dysregulation of its target genes. Some common observations involving CTCF function in cancers include the transcriptional activation of TERT, c-MYC, FOXM1, PLK, GAD1 and other genes [14, 22, 24–26] and the transcriptional repression of p53, BCL6, RASSF1A, CDH1 and others [27–30]. Additionally, chromatin immunoprecipitation (ChIP)-PCR analysis revealed that CTCF affects a number of metastasis-associated genes, including CTBP1, SERPINE1 and SRC [31]. Interestingly, a previous study showed that CTCF has one of the highest mutation rates in CRC [32]. However, the functional role of CTCF in CRC remains unclear.

In the present study, we observed abnormal CTCF expression in CRC. Additionally, we provided the first evidence of CTCF involvement in the P53-Hedgehog signaling pathway and confirmed the effects of aberrant CTCF expression on the cellular biological behavior, including proliferation and chemotherapy resistance to 5-fluorouracil (5-FU), of CRC cells *in vitro* as well as on tumor growth *in vivo*.

RESULTS

CTCF is a potential tumor-promoting gene in CRC

An online bioinformatics analysis website, Gene Expression Profiling Interactive Analysis (GEPIA, <http://gepia.cancer-pku.cn/>) [33], was used to explore the expression of CTCF in The Cancer Genome Atlas (TCGA) database, and the results indicated that CTCF was almost upregulated in all gastrointestinal tumors (Figure 1A). We divided CRC patients into two groups according to CTCF expression levels. Kaplan-Meier (K-M) survival analysis with PROGgeneV2 (<http://genomics.jefferson.edu/proggene/>) showed that the relapse-free survival time of patients with a high CTCF expression level was significantly shorter than that of patients with a low CTCF expression level in GSE31598 (Figure 1B). Analyses of CTCF-regulated gene set signatures with gene set enrichment analysis (GSEA) indicated that there is a positive correlation between high expression of CTCF and CRC gene set signatures (GSE17538 and TCGA, Figure 1C). Then, we assessed the expression level of CTCF in tumor and paracancerous normal colorectal tissues. CTCF expression in tumor and adjacent normal tissues was analyzed by qRT-PCR and western blot assays (Figure 1D, 1E), and the results showed that CTCF was upregulated in tumor specimens.

To further explore the function of CTCF *in vitro*, we examined CTCF expression in a human embryonic kidney cell line (293T), a human normal colon epithelial cell line (FHC) and six human CRC lines (SW480, SW620, RKO, HCT116 HT29 and LOVO). The expression level of CTCF was relatively high in SW480 cells and was comparatively low in the HCT116 cell line, which was confirmed by both qRT-PCR and western blot analyses (Supplementary Figure 1A, 1B). Herein, we selected SW480 and RKO cell lines to knock down endogenous CTCF expression. On the other hand, HCT116 and RKO cell lines were used to construct cell lines that stably overexpressed CTCF.

Overexpression of CTCF promotes human CRC cell proliferation

As a transcription factor, CTCF has been confirmed to play an essential role in the progression of multiple cancers [13]. To explore the role of CTCF in CRC, GSEA was performed to analyze the relationship between CTCF expression and cell cycle-relevant gene set signatures, and the results revealed that CTCF might promote cell proliferation (Figures 2A, 3A). As mentioned above, we chose two CRC cell lines (HCT116 and RKO) to construct CTCF-overexpressing cell lines via lentivirus infection. Transfection efficiency was assessed by green fluorescent protein (GFP) (Supplementary Figure 1C). Overexpression effect was confirmed by qRT-PCR (Figure 2B) and western blot (Figure 2C) analyses. CCK-8 and colony formation assays suggested that CTCF upregulation enhanced the proliferative ability in both CRC cell lines (Figure 2D, 2E and Supplementary Figure 1D). In addition, the EdU incorporation assays further confirmed that upregulated CTCF increased the proportion of EdU-positive cells (Figure 2F, 2G).

To investigate whether CTCF is involved in promoting human CRC cell growth *in vivo*, HCT116-CTCF cells and HCT116-Vector cells were subcutaneously injected into the right and left back hips of nude mice (n = 4/group). As shown (Figure 2H, 2I and Supplementary Figure 1E), the tumors in the CTCF-overexpressing group grew more rapidly than the control group tumors. Immunohistochemical (IHC) staining of Ki67 (Figure 2J) further demonstrated that the tumors in the CTCF-overexpressing group displayed much more proliferation than those in the control group.

Downregulation of CTCF impairs the proliferative capacity of human CRC cells

As previously mentioned, the SW480 cell line, which had the highest CTCF expression level, and RKO cell line were transfected with CTCF-specific shRNA to

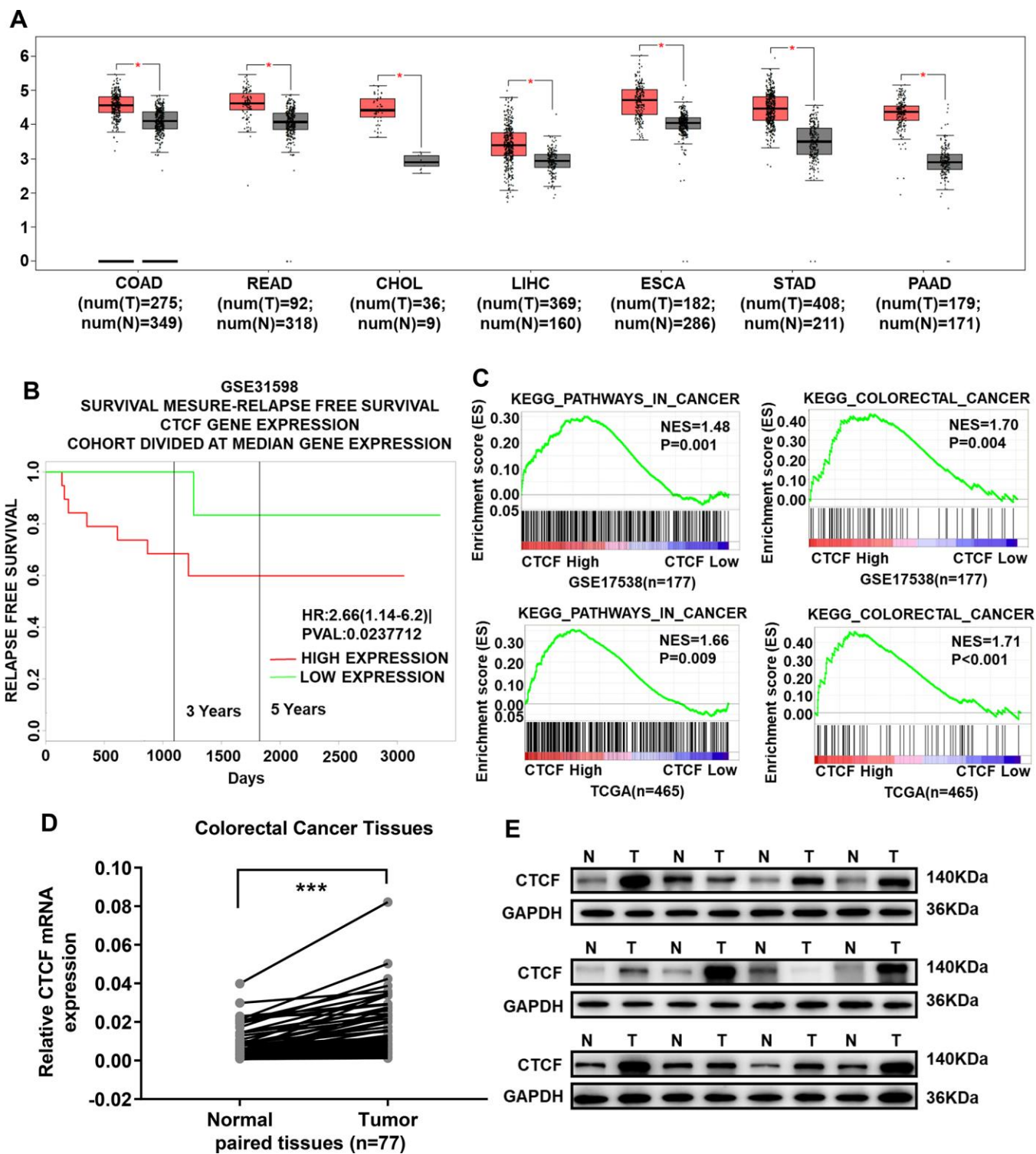


Figure 1. CTCF is significantly upregulated in CRC tissues and acts as a potential oncogenic gene. (A) CTCF is upregulated in all gastrointestinal tumors (GEPiA, <http://gepia.cancer-pku.cn/>). (B) Kaplan-Meier relapse free survival analysis in CRC patients with high or low expression of CTCF in GSE31598 via online website PROGgeneV2 (<http://genomics.jefferson.edu/proggene/>). (C) GSEA indicated that high expression of CTCF was positively correlated with the cancer related gene set signatures (KEGG_PATHWAYS_IN_CANCER, KEGG_COLORECTAL_CANCER) in CRC patient gene expression profiles (GSE17538, n = 177, and TCGA, n = 465). (D) qRT-PCR analysis of CTCF expression in 77 pairs of CRC patient specimens. (E) Western blot analyses of CTCF in 12 pairs of tumor and match adjacent normal tissues collected from clinical CRC patients. N for Normal, T for Tumor. The above data are presented as mean \pm SEM. * $P < 0.05$, ** $P < 0.01$, and *** $P < 0.001$.

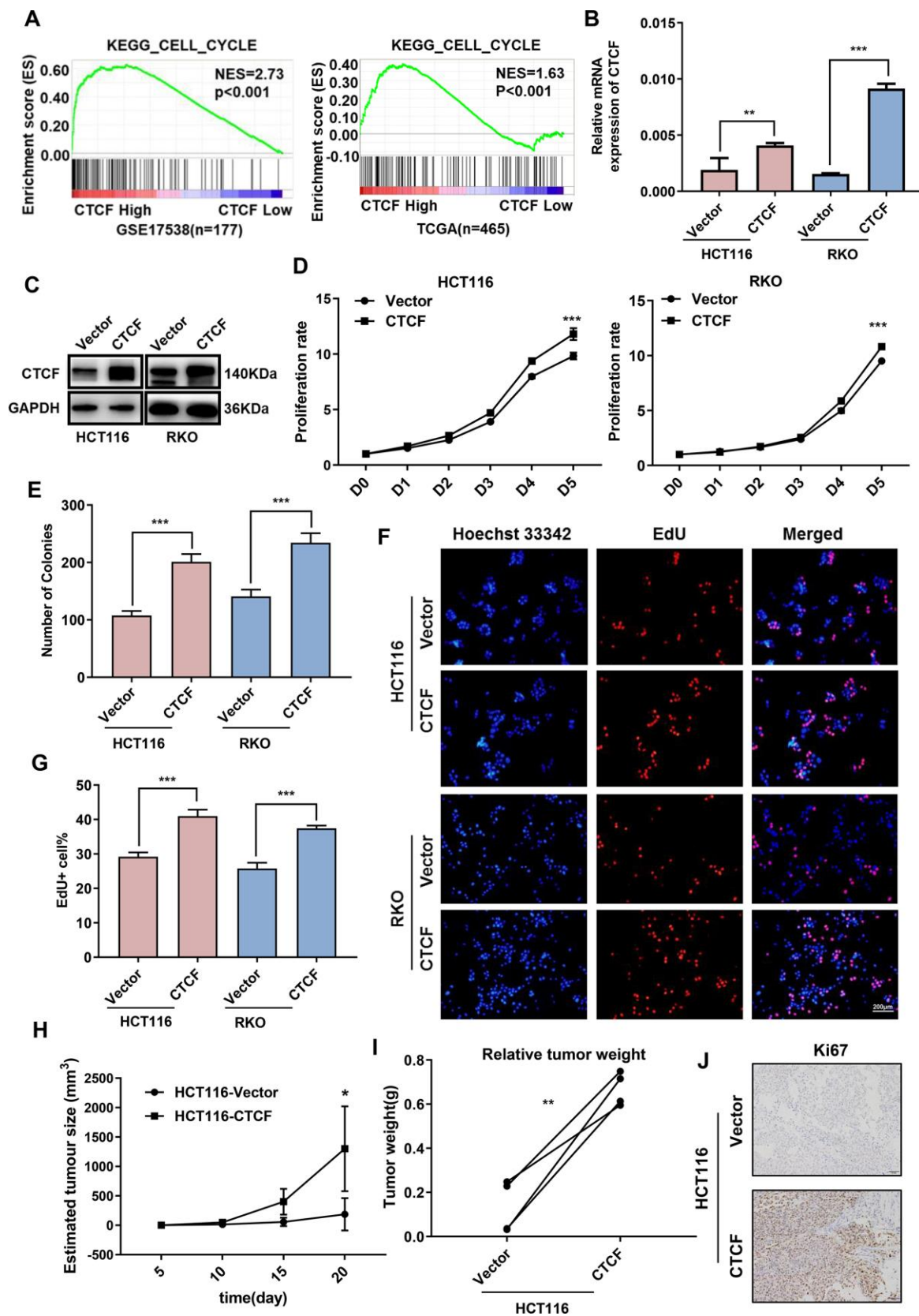


Figure 2. Upregulation of CTCF promotes human CRC cells proliferation. (A) GSEA plot indicated that high expression of CTCF is positively correlated with the cell cycle gene set signatures (KEGG_CELL_CYCLE) in published CRC patient gene expression profiles (GSE17538, n = 177, and TCGA, n = 465). (B, C) qRT-PCR and western blot analyses of CTCF expression level in constructed cell lines (HCT116 and RKO).

(D, E) The relative growth rates were measured using CCK8 and colony formation assays and compared between CTCF overexpressed group and Vector group at indicated times in HCT116 and RKO cell lines. (F) Images of EdU staining in both indicated cell lines, and the relative percentage of EdU-positive cells in images of related groups are shown (G). (H, I) Tumor volume and weight were measured and analyzed. (J) The tumor sections were under IHC staining using antibody against Ki-67. The above data are presented as mean \pm SEM. * $P < 0.05$, ** $P < 0.01$, and *** $P < 0.001$.

knockdown endogenous CTCF expression. Similarly, lentiviral infection efficiency was assessed by GFP (Supplementary Figure 2A). Knockdown effect was confirmed by qRT-PCR (Figure 3B) and western blot (Figure 3C) analyses. CCK-8 (Figure 3D), colony formation (Figure 3E and Supplementary Figure 2B) and EdU incorporation assays (Figure 3F, 3G) revealed that the downregulation of endogenous CTCF impaired the proliferative ability in both CRC cell lines. Furthermore, subcutaneous tumorigenesis in nude mice consistently showed that tumors in the SW480-shCTCF group grew much more slowly than the SW480-Scramble group (Figure 3H–3J and Supplementary Figure 2C). Besides, CTCF expression was positively correlated with the expression of CDKs and Cyclins in GEPIA (<http://gepia.cancer-pku.cn/>, Supplementary Figure 2D).

Thus, these results strongly suggested that CTCF increases the proliferative capacity of CRC cells *in vitro* and *in vivo*.

CTCF induces chemoresistance in CRC

Furthermore, to explore the possible role of CTCF in chemotherapy resistance, Cell growth inhibition rate was detected after treatment with a concentration gradient of 5-FU, and the results demonstrated that CTCF weakened the cytostatic action of 5-FU (Figure 4A, 4B). Cell apoptosis rate was determined by an apoptosis kit and flow cytometry. The apoptosis rate was increased in the CTCF knockdown group, while it was dramatically decreased in the CTCF-overexpressing group during treatment with 5-FU (Figure 4C and Supplementary Figure 3A, 3B). In addition, we investigated the protein expression level of CTCF and found that CTCF was significantly upregulated after treatment with 5-FU (10 μ M) in the HCT116 and RKO cell lines (Figure 4D). Consistently, the expression levels of crucial proteins in the apoptosis pathway were obviously reduced in the CTCF-overexpressing group, while they were increased in the CTCF-knockdown group (Figure 4E).

In further evaluations, the expression of ABCG2, which is a part of the superfamily of ATP-binding cassette (ABC) transporters and plays an important role in the chemotherapy resistance in various tumors [34], was positively related to CTCF expression (Figure 4F). Additionally, clinical specimens further confirmed there was a positive correlation between CTCF and ABCG2 (Figure 4G and Supplementary Figure 3C).

CTCF enhances malignant behavior in CRC via the Hedgehog signaling pathway

Previous studies reported that Hedgehog signaling pathway activation was closely associated with aggressive phenotypes and chemotherapy resistance in multiple malignancies, including lung cancer [35], pancreatic cancer [36], bladder cancer, etc. [37]. Hence, we examined whether there was a connection between CTCF and the Hedgehog signaling pathway. GSEA was performed to explore CTCF-regulated gene set signatures. The results demonstrated that “GCNP_SHH_UP_EARLY.V1_UP” and “GCNP_SHH_UP_LATE.V1_UP” and “GCNP_GLI1_UP.V1_UP” gene signatures enrich in the CTCF high expression group and “GCNP_SHH_UP_LATE.V1_DN” gene set enriches in the CTCF low expression group (GSE17538 and TCGA, Figure 5A). Then, we carried out western blot assays to investigate whether CTCF can activate Hedgehog signaling pathway in CRC. The results revealed that the expression levels of GLI1, Shh, PTCH1, and PTCH2 were increased in stable CTCF-overexpressing cell lines, while consistent phenomena was observed in the knockdown groups (Figure 5B). Also, correlation analysis in GEPIA revealed that CTCF was positively correlated with GLI1, Shh, PTCH1, and PTCH2 (Supplementary Figure 4A). K-M survival analysis with GEPIA revealed that high expression of GLI1 was accompanied by a shorter overall survival time (Supplementary Figure 4B). Moreover, GDC-0449, a Hedgehog signaling pathway inhibitor, was used for rescue assays, and western blot analyses showed that GDC-0449 counteracted the CTCF-induced activation of the Hedgehog signaling pathway (Figure 5B).

Subsequently, we explored whether the direct blockade of the Hedgehog signaling pathway could restore the function CTCF plays in CRC cell lines. Consistently, we found that treatment with GDC-0449 reversed the enhanced proliferation ability, which was induced by CTCF, based on CCK-8 (Figure 5C) and EdU staining assays (Figure 5D–5F).

CTCF activates the Hedgehog signaling pathway via transcriptional repression of P53

To predict the potential target genes involved in chemotherapy resistance to 5-FU, 3 bioinformatic target prediction programs (PubChem, STICH, and SuperPred Target-Prediction) were used to explore putative targets

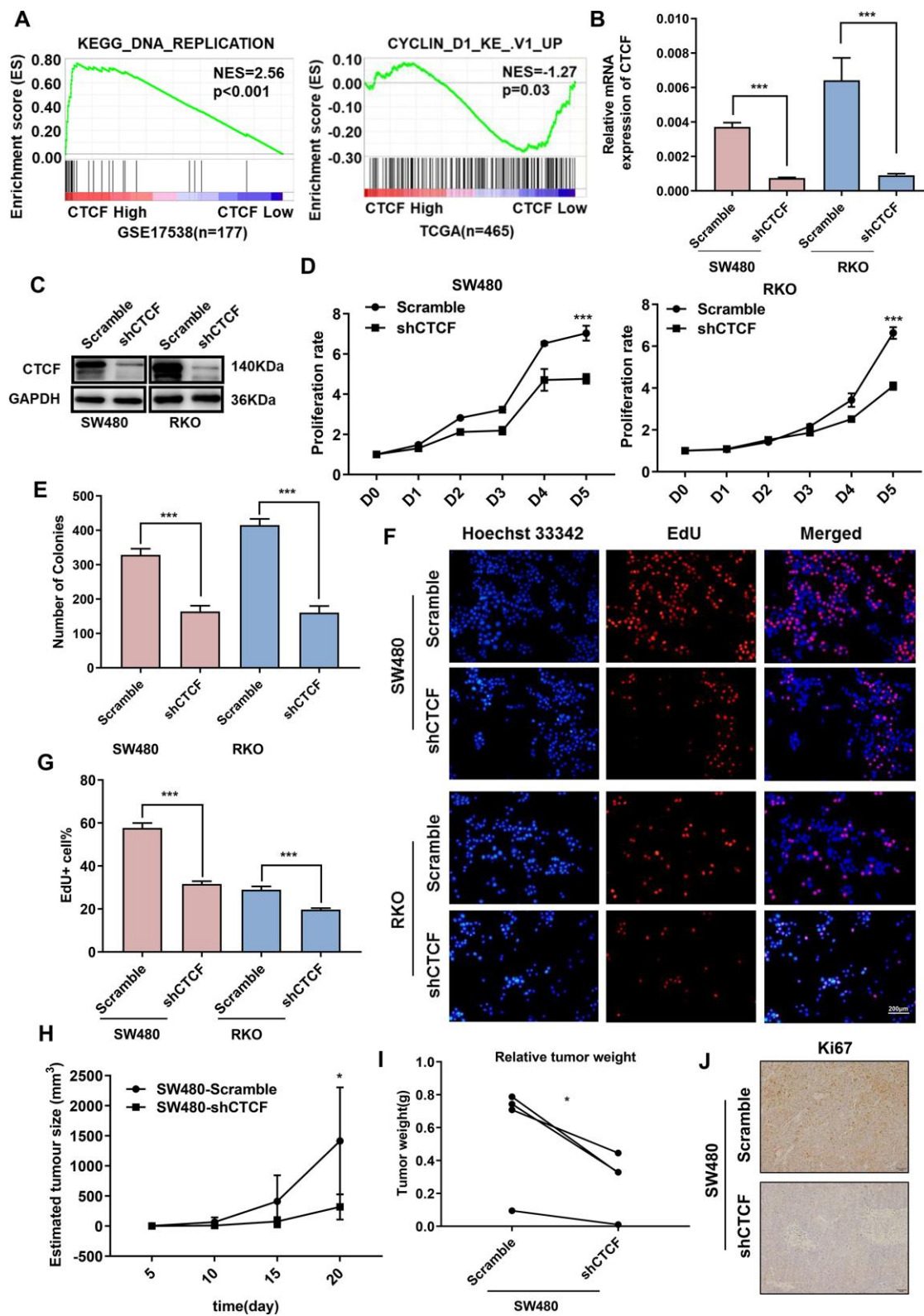


Figure 3. Inhibition of CTCF represses human CRC cells proliferation. (A) GSEA results showed that “KEGG_DNA_REPLICATION” gene set enriches in the CTCF high expression group and “CYCLIN_D1_KE_V1_UP” gene set enriches in the CTCF low expression group (GSE17538, n = 177, and TCGA, n = 465). (B, C) qRT-PCR and western blot analyses of CTCF expression level in the constructed cell lines (SW480 and RKO). (D–G) Cell reproductive capacity was examined by CCK8, colony formation and EdU staining assays. (H, I) Tumor volume and weight of subcutaneous tumor were measured and analysed. (J) Immunohistochemistry was performed to determine Ki-67 expression. The above data are presented as mean ± SEM. * P<0.05, **P<0.01, and ***P<0.001.

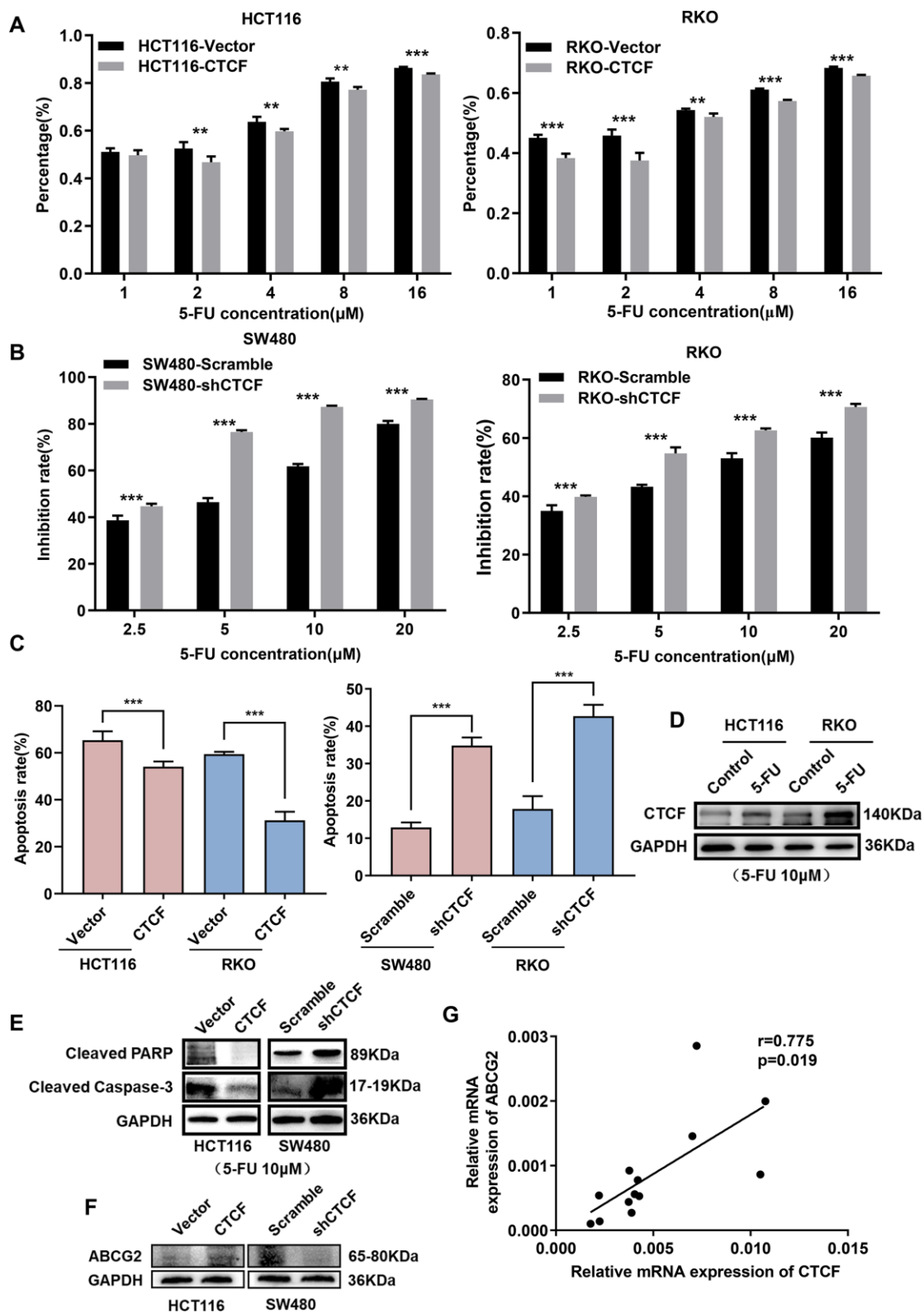


Figure 4. CTCF induces 5-FU-based chemoresistance in CRC. (A, B) Cell growth inhibition rate was measured via CCK8 analysis and compared between different groups with different treatment concentration at indicated time (48 hours). (C) The apoptosis rate of different transfected groups with 5-FU treatment were measured by flow cytometry. (D) Western blot analysis of CTCF in HCT116 and RKO cell lines after 5-FU (10 μM) treatment for 48 hours. (E, F) Western blot analyses of cleaved-PARP, cleaved Caspase-3 and ABCG2 in HCT116 and SW480 cell lines. (G) Spearman correlation analyses between relative CTCF and ABCG2 mRNA expression in 13 fresh human CRC specimens. The above data are presented as mean \pm SEM. * $P < 0.05$, ** $P < 0.01$, and *** $P < 0.001$.

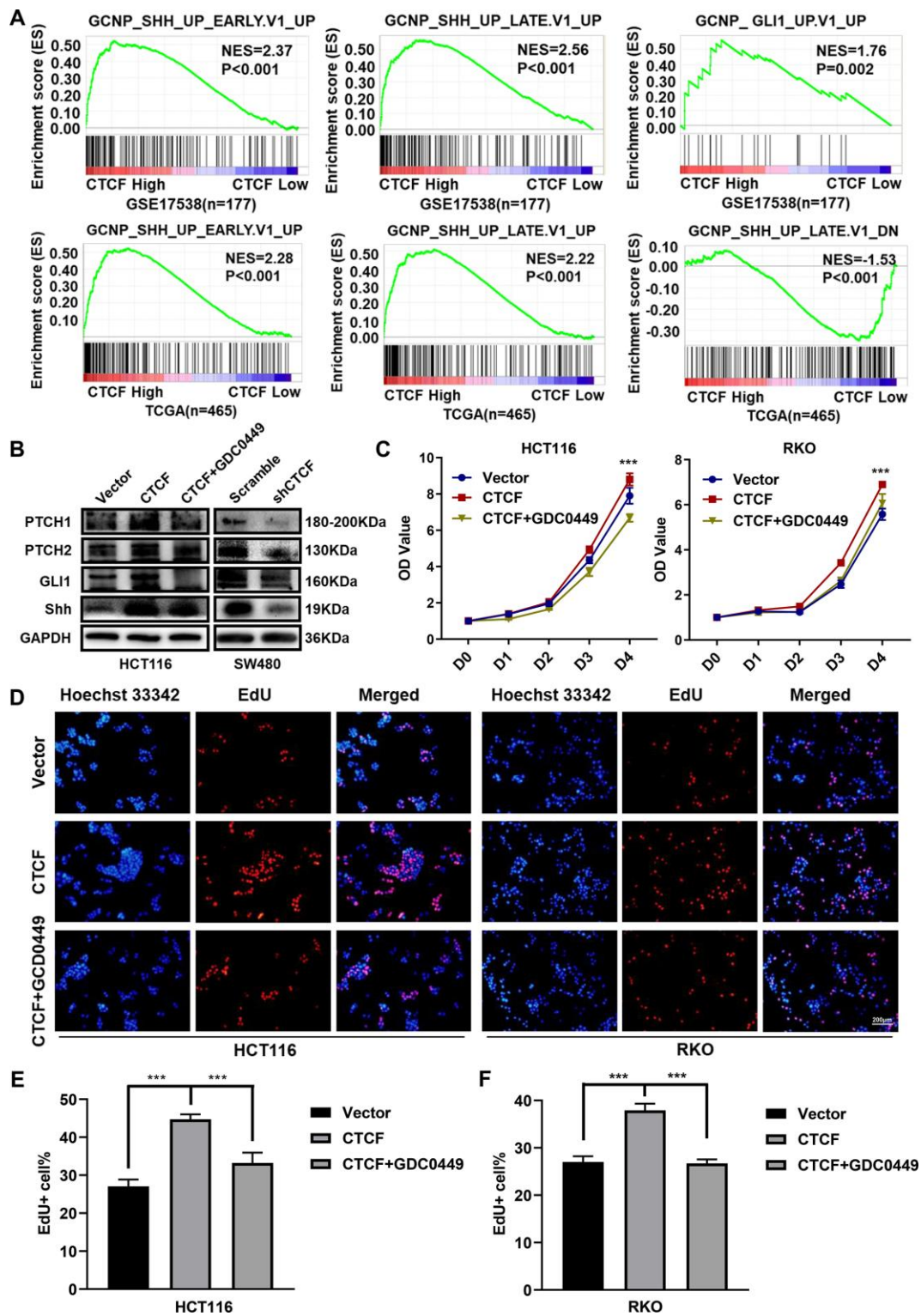


Figure 5. CTCF activates Hedgehog signaling pathway. (A) GSEA plots indicated that “GCNP_SHH_UP_EARLY.V1_UP” and “GCNP_SHH_UP_LATE.V1_UP” and “GCNP_GLI1_UP.V1_UP” gene signatures enrich in the CTCF high expression group and “GCNP_SHH_UP_LATE.V1_DN” gene set enriches in the CTCF low expression group (GSE17538, n = 177, and TCGA, n = 465). (B) Western blot analyses of Key molecules of Hedgehog signaling pathway in different transfected groups with or without the stimulation of Hedgehog signaling pathway inhibitor, GDC-0449 (2 μ M). (C) Relative growth rate of different transfected groups with or without the administration of GDC-0449 (2 μ M). (D–F) Images of EdU staining of both indicated cell lines with or without the administration of GDC-0449, and the relative percentage of EdU-positive cells in images of related groups is shown. The above data are presented as mean \pm SEM. * P<0.05, **P<0.01, and ***P<0.001.

of 5-FU. Venn diagram enrichment analysis showed that TYMS and TP53 were theoretical target genes of 5-FU (Figure 6A). Then, we analyzed the interactions among CTCF, the above two target genes and the key molecules of the Hedgehog signaling pathway in functional protein association networks (STRING, <https://string-db.org/>, Figure 6B), the results suggested that P53 may be a “bridge” between CTCF and the Hedgehog signaling pathway. GSEA plots showed that CTCF was negatively correlated with P53-related gene set signatures (GSE17538, $n = 177$, Figure 6C). Moreover, GO enrichment were performed to analyze the top 30 similar genes of CTCF in GEPIA (<http://gepia.cancer-pku.cn/>). As the bubble diagram shown (Supplementary Figure 5A), “p53 binding” was in the top 20 of GO enrichment. qRT-PCR analyses showed that CTCF repressed P53 expression (Figure 6E). K-M survival analysis with GEPIA revealed that high expression of TP53 was accompanied by a longer survival time (Supplementary Figure 5B). Interestingly, high ratio of CTCF/TP53 was accompanied by a shorter disease free survival time while the prognosis of the high TP53/CTCF ratio group was good (Supplementary Figure 5C). A previous study [27] identified CTCF binding site (CBS) in the promoter region approximately 800 bp upstream of the P53 transcription start site (Figure 6D). Therefore, ChIP-qPCR and ChIP-PCR assays were performed to confirm whether CTCF can bind to the site in CRC (Supplementary Figure 6A and Figure 6F). Moreover, a dual luciferase reporter assay showed that the knockdown of CTCF enhanced P53 luciferase activity (Figure 6G). Clinical specimens further confirmed that there was a negative correlation between CTCF and P53 (Supplementary Figure 6B).

To further validate whether CTCF activates the Hedgehog signaling pathway via P53, siRNA targeting P53 was used for rescue assays. Western blot assays demonstrated that the knockdown of P53 counteracted the CTCF knockdown-induced repression of the Hedgehog signaling pathway (Figure 6H). Nuclear extract assays revealed that the inhibition of P53 blocked the CTCF knockdown-induced intranuclear reduction of GLI1 (Figure 6I, 6J). In addition, a colony formation assay showed that the decrease of P53 impaired changes in proliferative capacity caused by CTCF knockdown (Supplementary Figure 6C).

CTCF-induced chemoresistance is dependent on the P53-Hedgehog axis

The above results showed that CTCF can block 5-FU-stimulated cell apoptosis and activate the Hedgehog signaling pathway via transcriptional repression of P53. However, further information is needed to determine whether the associations are causal. Apoptosis assays

indicated that administration of GDC-0449 dramatically increased 5-FU-stimulated cell apoptosis rate repressed by overexpression of CTCF (Figure 7A and Supplementary Figure 6D). Western blot analysis revealed that P53 restored the ABCG2 increase induced by CTCF (Figure 7B). Moreover, an *in vivo* tumor growth assay confirmed that the inhibition of the Hedgehog signaling pathway with JK184 recovered the stimulation of cell proliferation caused by upregulated CTCF ($n=5$ /group, Figure 7D, 7E).

DISCUSSION

CRC is one of the most lethal cancers worldwide. Although progress has been made in CRC diagnosis and treatments, the prognosis of some CRC patients is still poor and is affected by chemotherapy resistance, postoperative recurrence, and metastasis [5, 38].

Studies have revealed that CTCF is robustly upregulated in several cancers and promotes the malignant characteristics of tumor cells [13, 18]. Moreover, Marois Giannakis et al. recently identified recurrently mutated genes in CRC, including TP53, KRAS, SMAD4, CTCF, etc., by performing whole-exome sequencing of 619 incident CRCs and integrating the results with tumor immunity, pathology, and survival data [32]. However, CTCF was not previously studied in CRC progression, which drove us to explore the exact role of CTCF in CRC. Herein, we demonstrated that CTCF was upregulated in CRC tissues by performing western blot and qRT-PCR assays. The overexpression of CTCF promoted malignant phenotypes in CRC by enhancing the proliferative potential and clonogenicity of CRC cells.

Although corresponding 5-FU-based chemotherapies, including FOLFIRI [39], FOLFOX [40], XELOX [41] and other regimens [38], have been developed in the past few years, the clinical outcome remains unsatisfactory, as some CRC patients suffer from chemotherapy resistance. Interestingly, our study indicated that CTCF overexpression reduced the sensitivity of CRC cells to 5-FU and decreased 5-FU-induced apoptosis, which offered a novel explanation for the emergence of chemoresistance in CRC. ABCG2 has been suggested to be involved in clinical multidrug resistance (MDR) in cancer [42], and we found that ABCG2 was activated by CTCF in CRC. Hence, the inhibition of CTCF might be a new strategy to support chemotherapy in CRC patients.

The Hedgehog signaling pathway is involved in many aspects of tumorigenesis and malignant characteristics, including cell cycle progression, proliferation, angiogenesis, migration, invasion, and, in particular, chemotherapy resistance [43, 44]. For example, the

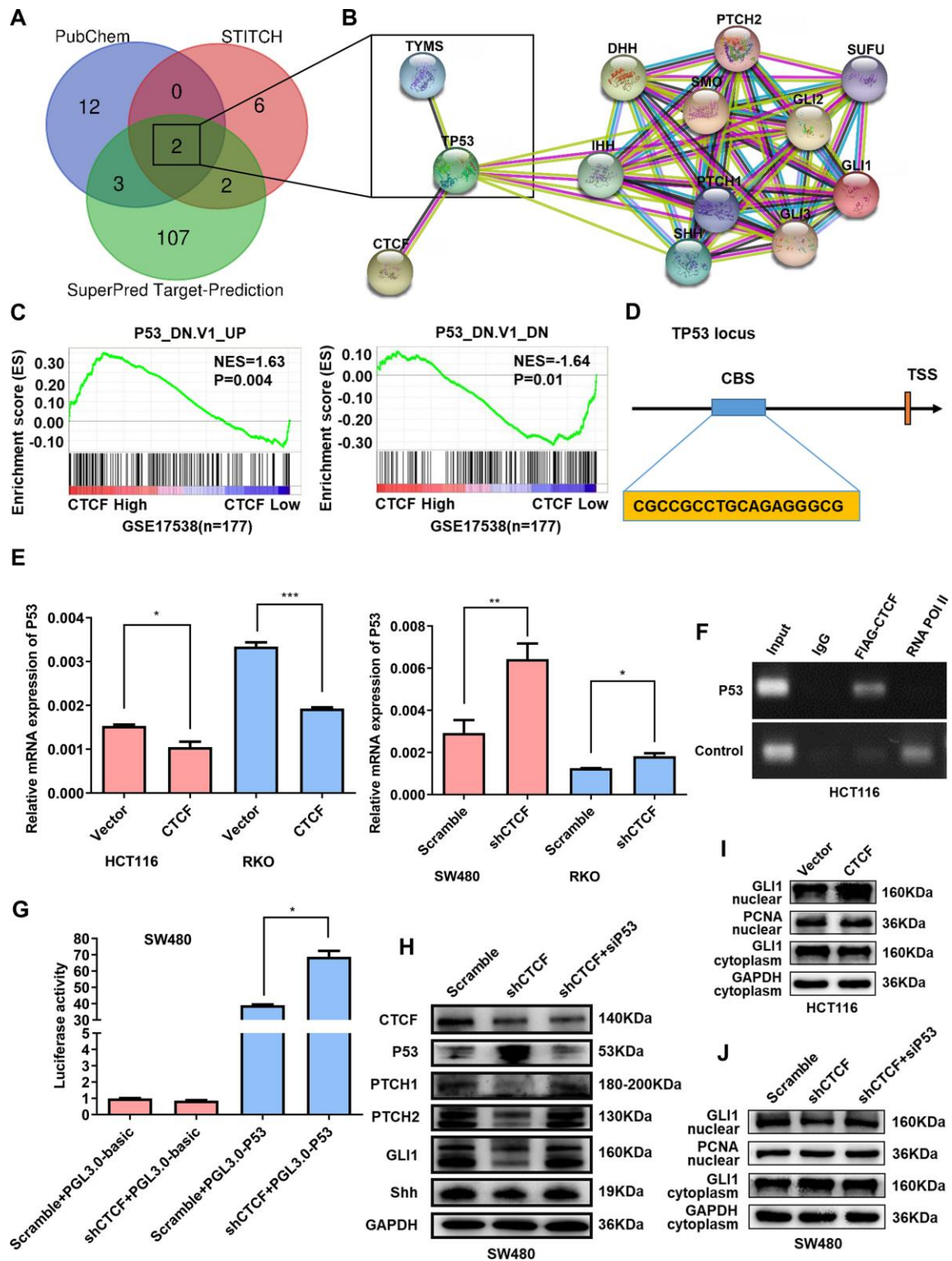


Figure 6. CTCF enhances Hedgehog signaling pathway activation via targeting P53. (A) Venn diagram enrichment analysis of the 5-FU putative target genes. (B) Protein-protein interaction analysis via STRING (<https://string-db.org/>). (C) GSEA plots indicated that “P53_DN.V1_UP” gene set signature enriches in the CTCF high expression group and “P53_DN.V1_DN” gene set enriches in the CTCF low expression group (GSE17538, n = 177). (D) Schematic view of the P53 gene transcription start site (TSS) with a CTCF-binding site (CBS). (E) qRT-PCR analysis of P53 expression level in constructed cell lines. (F) ChIP-PCR results for CTCF on the CBS in HCT116 cells. (G) P53 luciferase reporter activity was analyzed in SW480 cells. (H) Western blot analysis of key molecules of Hedgehog signaling pathway and P53 in different transfected groups with or without the stimulation of P53-specific siRNA. (I, J) Nuclear extract assays and western blot analyses of GLI1 in indicated cells. The above data are presented as mean \pm SEM. * $P < 0.05$, ** $P < 0.01$, and *** $P < 0.001$.

persistent activation of the Hedgehog pathway was confirmed to play a critical role in the chemoresistance and prognosis of cancer patients [45]. In addition, ABCG2 is a direct transcriptional target of the Hedgehog signaling pathway and is involved in drug tolerance in diffuse large B-cell lymphoma [46]. Hence, we performed GSEA to analyze the relationship between CTCF and the Hedgehog signaling pathway and found that the enrichment of Hedgehog pathway-related gene

set signatures is notably related to CTCF expression. Furthermore, our results showed that the overexpression of CTCF increased GLI1, Shh, PTCH1, and PTCH2 levels, while silencing CTCF induced low GLI1, Shh, PTCH1, and PTCH2 expression. Additionally, the administration of the Hedgehog signaling pathway inhibitor GDC-0449 counteracted the increased proliferation and clonogenicity induced by CTCF up-regulation. Furthermore, rescue assays, including

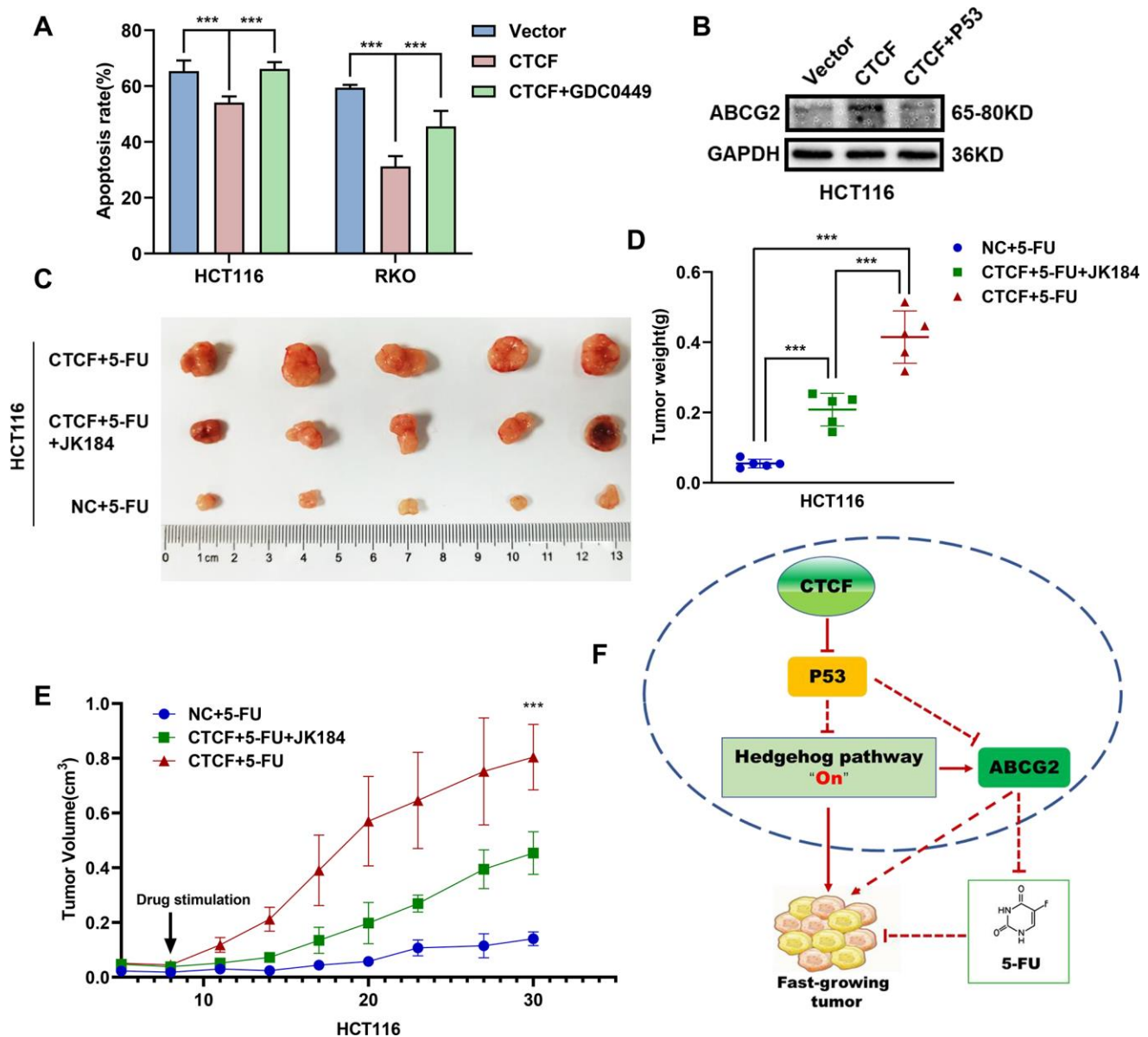


Figure 7. CTCF promotes chemoresistance by regulating P53-Hedgehog axis signaling. (A) Apoptosis assays showed the effect of GDC0449 on CTCF-mediated 5-FU stimulated apoptosis of CRC cells. (B) Western blot analysis of the effects of P53 on CTCF-mediated ABCG2 upregulation. (C) The representative images of subcutaneous tumors from different experimental groups are shown. (D, E) Tumor weight and volume analyses showed that JK184 recovered the stimulative cell proliferation caused by upregulated CTCF under stimulation of 5-FU. (F) A hypothetical model illustrating that CTCF transcriptionally represses P53 and activates the Hedgehog signaling pathway to promote proliferation and 5-FU chemotherapy resistance of CRC cells. The above data are presented as mean \pm SEM. * $P < 0.05$, ** $P < 0.01$, and *** $P < 0.001$.

in vivo tumor growth assays and apoptosis assays, demonstrated that CTCF sustains CRC proliferation and chemotherapy resistance by activating the Hedgehog signaling pathway. However, the mechanism by which CTCF activates the Hedgehog signaling pathway is still unclear.

Thus, the above results indicated that CTCF promotes CRC proliferation and chemotherapy resistance via the Hedgehog signaling pathway. The mechanism by which CTCF activates the Hedgehog signaling pathway needs to be clarified, as previous studies have not reported this relationship. Through network pharmacologic analysis, we found that P53 and TYMS are the potential key target genes of 5-FU. In recent years, more and more studies have shown that TYMS and P53 are crucial molecules in 5-FU resistance [47, 48]. Furthermore, we found P53 might be a key molecule that connects CTCF and the Hedgehog signaling pathway by constructing a protein interaction network. P53 is a crucial molecule in the progression of virtually every malignant tumor [49]. Furthermore, it has been reported that P53 can suppress the Hedgehog signaling pathway [50]. GSEA revealed that CTCF expression is closely related to P53-related gene set signatures. A previous study reported that CTCF transcriptionally inhibits P53 in breast cancer [27]. Hence, we performed qRT-PCR, ChIP and dual luciferase reporter assays to investigate whether the regulatory mechanism between CTCF and P53 also exists in CRC cells. The results showed that CTCF can inhibit P53 transcription via bind to the promoter region of P53.

As mentioned above, studies showed that P53 can suppress the Hedgehog signaling pathway, and our study revealed that CTCF transcriptionally repressed P53 expression. Protein interaction network revealed that P53 is a “bridge” connecting CTCF to Hedgehog signaling pathway. However, whether CTCF activates Hedgehog signaling pathway is P53 dependent in CRC still should be clarified. Hence, we performed rescue assays, including western blot and nuclear extract assays, to investigate the relationship among CTCF, P53 and Hedgehog signaling pathway. Western blot assays demonstrated that CTCF activates the Hedgehog signaling pathway through the repression of P53. Furthermore, nuclear extract assays demonstrated that P53 repression increases the nuclear accumulation of GLI1 which is induced by CTCF. Most of all, subcutaneous xenotransplanted tumor model of human CRC in nude mice further confirmed that CTCF enhanced 5-FU resistance via activating Hedgehog signaling pathway.

In summary, our work provides evidence that CTCF facilitates malignant properties and induces chemotherapy resistance to 5-FU in CRC by regulating the

P53-Hedgehog axis. This work introduces a potential biomarker for CRC and a therapeutic target to reduce chemoresistance in patients with CRC.

MATERIALS AND METHODS

Clinical specimens and cell culture

With approval from the institutional review board of the hospital ethics committee (Nanfang Hospital, Southern Medical University), clinical CRC specimens and matched normal tissues were collected from 90 patients who underwent surgical treatment for CRC at Nanfang Hospital of Southern Medical University after obtaining informed consent. Additionally, the study was conducted in accordance with the Declaration of Helsinki. CRC was histopathologically confirmed in each patient. Cancer tissues and adjacent normal tissues were frozen at -80°C for storage.

A human embryonic kidney cell line (293T), human normal colon epithelial cell line (FHC) and six human CRC cell lines (SW480, SW620, RKO, HCT116 HT29 and LOVO) were purchased from the Cell Bank of Type Culture Collection (CBTCC, Chinese Academy of Sciences, Shanghai, China) and were cultured in DMEM (Gibco, Carlsbad, CA) supplemented with 10% fetal bovine serum (Gibco, Carlsbad, CA). Cells were maintained at 37°C in a humidified atmosphere with 5% CO₂.

Plasmid construction, lentiviral construction and cell transfection

The overexpression and downregulation of CTCF were achieved by lentiviral delivery. To construct CTCF-overexpressing cell lines, full-length CTCF (NM_006565) was cloned into the expression vector pLenti-EF1a-EGFP-P2A-Puro-CMV (Obio Technology, Shanghai, China) and transfected into HCT116 and RKO cell lines according to the manufacturer's instructions. The knockdown of CTCF was accomplished with shRNA (Cyagen, Guangzhou, China) that were transfected into SW480 and RKO cell lines according to the manufacturer's instructions. The CTCF shRNA sequence was sense 5'-GCGAAAGCAGCATTCCCTA TAT-3', and the scrambled sequence was sense 5'-CCTAAGGTTAAGTCGCCCTCG-3'. Transduced cells were selected in medium containing puromycin (#EZ2811D376, BioFrox, China) (2 µg/ml) and maintained in medium containing puromycin (1 µg/ml).

Plasmid and siRNA transfection

To exogenously overexpress TP53, full-length TP53 (NM_000546.6) was cloned into the expression vector

pENTER (Vigene, Shandong, China). The knockdown of TP53 was achieved by siRNA (Genecopoeia, Shanghai, China). The TP53 siRNA sequence was sense 5'-GAAGAAACCACUGGAUGGATT -3', and the negative control sequence was sense 5'-UUCUCCGAACGUGUCACGUTT-3'. Genomic DNA fragments from the TP53 locus (-1000-0 bp of the TP53 promoter region) were cloned into the pGL3-basic vector (Obio Technology, China). Plasmids or siRNA were transfected into CRC cells with LipofectamineTM 3000 (Invitrogen, Carlsbad, CA) according to the manufacturer's instructions.

Cell Counting Kit-8 (CCK-8), colony formation assays

CCK-8 (Dojindo, Japan) analysis was used to estimate cell proliferation. The transfected cell lines were cultured on the 96-well plates and then with culture medium containing 10ul CCK-8 each well and incubated for 2 hours. Proliferation was determined by absorbance measurement at 450 nm using a microplate reader.

Cells were seeded in 6-well plates at a density of 5×10^2 per well and incubated at 37 °C in a humidified atmosphere with 5% CO₂ and the medium was replaced every 3-4 days. The colonies were counted and analysed in about two weeks. The experiment was performed with at least three replicates for each cell line.

5-Ethynyl-2'-deoxyuridine (EdU) incorporation and apoptosis assays

As the manufacturer's instructions for a Cell-Light EdU DNA cell proliferation kit (#C103010-1, RiboBio, China) described, transfected cell lines were seeded in 96-well plates and incubated with EdU in medium (50 μM) for 2 hours. Then, cells were washed twice and fixed in 4% paraformaldehyde for 10 min, permeabilized with 0.5% Triton-X 100, and stained with Apollo® fluorescent dye. Photographs of cells were independently taken with an OLYMPUS confocal microscope.

The cells were analyzed by FACS according to the standard protocol provided by the manufacturer (BD FACSAria II). Apoptosis was measured by using an Annexin V-PE/7-Amino-Actinomycin (7-AAD) Apoptosis Detection Kit (#559763, BD Biosciences Pharmingen, US). After treatment with 5-FU (#9648, TargetMol, China) at the indicated concentrations for 48 hours, cells were harvested by trypsinization, washed with cold PBS and then resuspended in 1X binding buffer. Then, 5 μl of PE Annexin V and 5 μl 7-AAD were added to each tube. The suspension was then mixed well and incubated for 15 min in the dark at room temperature (RT) (25°C). After resuspension, samples were analyzed by flow cytometry.

RNA isolation, cDNA synthesis, and quantitative real-time PCR (qRT-PCR)

Total RNAs were extracted from cells or fresh surgical CRC tissues with Trizol solution (TaKaRa). Quantitative real-time polymerase chain reaction (qRT-PCR) was performed in triplicate using the PrimeScript RT Reagent Kit, SYBR Premix Ex Taq (TaKaRa) and a Roche Light Cycler 480 Real-Time PCR System (Roche Diagnostics, Mannheim, Germany) following the manufacturer's instructions. Relative gene expression levels were normalized to the expression of GAPDH. qRT-PCR results were analyzed to obtain Ct values of amplified products, and data was analyzed by the 2- $\Delta\Delta$ Ct method. The specific primers used for detection are listed in Supplementary Table 1.

Western blot and immunohistochemistry (IHC)

We performed western blot according to the previous study [51]. Protein lysates were prepared, subjected to SDS-PAGE, transferred onto PVDF membranes and blotted according to standard methods by using following antibodies: CTCF(#2899, Cell Signaling), PTCH1 (#2648, Cell Signaling), and PTCH2 (#2470, Cell Signaling), GLI1(#3538, Cell Signaling), Shh(#2207, Cell Signaling), GAPDH (60004-1-Ig, Proteintech), Cleaved PARP (BF9106, Affinity), Cleaved Caspase-3 (# 9661S, Cell Signaling), TP53 (AF0879, Affinity), ABCG2 (#42078T, Cell Signaling).

Immunohistochemistry was performed following the manufacturer's instructions (PV-6001, ZSGB-BIO, Beijing, China) and used the antibody (anti-Ki67, 27309-1-AP, Proteintech)

ChIP and dual luciferase reporter assays

ChIP assays were performed with a kit (#17-10085, Merck) as previously described [51]. The CTCF binding site (CBS) at the transcriptional start site of TP53 was amplified with qRT-PCR and PCR. The specific primers are included in Supplementary Table 1. Luciferase activity was detected with a dual luciferase assay kit (Promega, America), as previously described [52].

Network pharmacologic analysis

List of websites used as follows, PubChem: <https://pubchem.ncbi.nlm.nih.gov/>, STITCH: <http://stitch.embl.de/>, SuperPred Target-Prediction: http://prediction.charite.de/index.php?site=chemdoodle_search_target, STRING: <https://string-db.org/>. The Canonical SMILES of 5-FU is C1=C(C(=O)NC(=O)N1)F, and the InChI Key of 5-FU is GHASVSINZRGABV-UHFFFAOYSA-N.

***In vivo* experiments**

Female athymic 4- to 5-week-old Balb/C (nu/nu) mice were purchased from the Laboratory Animal Services Centre of Guangdong Province and were maintained in a specific pathogen-free facility. For the tumor growth assay, 5×10^6 cells were subcutaneously injected into the right and left back of nude mice (n=4/group). For drug treatment assays, 1×10^7 cells were subcutaneously injected into the right back of nude mice (n=5/group). JK184 (5 mg/kg body weight, #315703-52-7, MCE) and 5-FU (23 mg/kg body weight, #51-21-8, MCE) were used to treat nude mice according to the manufacturer's instructions. The tumor volume was calculated using the following formula: $V = 0.5 \times D \times d^2$ (V represents volume, D represents the longitudinal diameter, and d represents the latitudinal diameter). The use of animals was approved by the Nanfang Hospital Animal Ethics Committee (ethical code NFYY-2018-38; approval date-10 April 2018).

Statistical analysis

All experiments were performed at least thrice. The SPSS 17.0 (SPSS; Chicago, IL, USA) statistical analysis software was used for statistical analysis of experimental data. The significance of differences between groups was estimated by Student's t-test. Additionally, multiple group comparisons were analyzed with one-way ANOVA. * $P < 0.05$, ** $P < 0.01$, and *** $P < 0.001$ were considered significant.

AUTHOR CONTRIBUTIONS

SDL and AML designed the experiments; QHL, QYL, CCH, YXF, SML, JQC and JD conducted experiments; YFL, YZ, XKW, QZ, JH and QY provided research materials and methods; QHL and QYL analyzed data; and QHL wrote the manuscript, SDL, AML and CJW reviewed the manuscript. All authors read and approved the final manuscript.

ACKNOWLEDGMENTS

We thank Junsheng Chen for helping us make a pathological diagnosis.

CONFLICTS OF INTEREST

The authors declare no conflicts of interest.

FUNDING

This study was supported by Guangdong Gastrointestinal Disease Research Center (No.2017B020209003), National Natural Science Funds of China (No.81772964),

China's Postdoctoral Science Fund (2019M663005) and the Foundation for the President of Nanfang Hospital of Southern Medical University (2018C027 and 2019B014).

Editorial note

&This corresponding author has a verified history of publications using the personal email addresses for correspondence.

REFERENCES

1. Brenner H, Kloor M, Pox CP. Colorectal cancer. *Lancet*. 2014; 383:1490–502.
[https://doi.org/10.1016/S0140-6736\(13\)61649-9](https://doi.org/10.1016/S0140-6736(13)61649-9)
PMID:[24225001](https://pubmed.ncbi.nlm.nih.gov/24225001/)
2. Inadomi JM. Screening for Colorectal Neoplasia. 1533-4406 (Electronic).
3. Siegel RL, Miller KD, Fedewa SA, Ahnen DJ, Meester RG, Barzi A, Jemal A. Colorectal cancer statistics, 2017. *CA Cancer J Clin*. 2017; 67:177–93.
<https://doi.org/10.3322/caac.21395>
PMID:[28248415](https://pubmed.ncbi.nlm.nih.gov/28248415/)
4. Pfister DG, Benson AB 3rd, Somerfield MR. Clinical practice. Surveillance strategies after curative treatment of colorectal cancer. *N Engl J Med*. 2004; 350:2375–82.
<https://doi.org/10.1056/NEJMcp010529>
PMID:[15175439](https://pubmed.ncbi.nlm.nih.gov/15175439/)
5. Xiong M, Zhuang K, Luo Y, Lai Q, Luo X, Fang Y, Zhang Y, Li A, Liu S. KIF20A promotes cellular Malignant behavior and enhances resistance to chemotherapy in colorectal cancer through regulation of the JAK/STAT3 signaling pathway. *Aging (Albany NY)*. 2019; 11:11905–21.
<https://doi.org/10.18632/aging.102505>
PMID:[31841120](https://pubmed.ncbi.nlm.nih.gov/31841120/)
6. Meyerhardt JA, Mayer RJ. Systemic therapy for colorectal cancer. *N Engl J Med*. 2005; 352:476–87.
<https://doi.org/10.1056/NEJMra040958>
PMID:[15689586](https://pubmed.ncbi.nlm.nih.gov/15689586/)
7. Kehlet H. Fast-track colorectal surgery. *Lancet*. 2008; 371:791–93.
[https://doi.org/10.1016/S0140-6736\(08\)60357-8](https://doi.org/10.1016/S0140-6736(08)60357-8)
PMID:[18328911](https://pubmed.ncbi.nlm.nih.gov/18328911/)
8. Maeda H, Kashiwabara K, Aoyama T, Oba K, Honda M, Mayanagi S, Kanda M, Hamada C, Sadahiro S, Sakamoto J, Saji S, Yoshikawa T. Hazard rate of tumor recurrence over time in patients with colon cancer: implications for postoperative surveillance from three Japanese foundation for multidisciplinary treatment of cancer (JFMC) clinical trials. *J Cancer*. 2017; 8:4057–64.
<https://doi.org/10.7150/jca.21365>
PMID:[29187881](https://pubmed.ncbi.nlm.nih.gov/29187881/)

9. Vecchione L, Gambino V, Raaijmakers J, Schlicker A, Fumagalli A, Russo M, Villanueva A, Beerling E, Bartolini A, Mollevi DG, El-Murr N, Chiron M, Calvet L, et al. A vulnerability of a subset of colon cancers with potential clinical utility. *Cell*. 2016; 165:317–30. <https://doi.org/10.1016/j.cell.2016.02.059> PMID:27058664
10. Ma S, Yang D, Liu Y, Wang Y, Lin T, Li Y, Yang S, Zhang W, Zhang R. LncRNA BANCR promotes tumorigenesis and enhances adriamycin resistance in colorectal cancer. *Aging (Albany NY)*. 2018; 10:2062–78. <https://doi.org/10.18632/aging.101530> PMID:30144787
11. Yan L, You WQ, Sheng NQ, Gong JF, Hu LD, Tan GW, Chen HQ, Wang ZG. A CREB1/miR-433 reciprocal feedback loop modulates proliferation and metastasis in colorectal cancer. *Aging (Albany NY)*. 2018; 10:3774–93. <https://doi.org/10.18632/aging.101671> PMID:30523220
12. Liao W, Overman MJ, Boutin AT, Shang X, Zhao D, Dey P, Li J, Wang G, Lan Z, Li J, Tang M, Jiang S, Ma X, et al. KRAS-IRF2 axis drives immune suppression and immune therapy resistance in colorectal cancer. *Cancer Cell*. 2019; 35:559–72.e7. <https://doi.org/10.1016/j.ccell.2019.02.008> PMID:30905761
13. Song SH, Kim TY. CTCF, cohesin, and chromatin in human cancer. *Genomics Inform*. 2017; 15:114–22. <https://doi.org/10.5808/GI.2017.15.4.114> PMID:29307136
14. Eldholm V, Haugen A, Zienolddiny S. CTCF mediates the TERT enhancer-promoter interactions in lung cancer cells: identification of a novel enhancer region involved in the regulation of TERT gene. *Int J Cancer*. 2014; 134:2305–13. <https://doi.org/10.1002/ijc.28570> PMID:24174344
15. Kim S, Yu NK, Kaang BK. CTCF as a multifunctional protein in genome regulation and gene expression. *Exp Mol Med*. 2015; 47:e166. <https://doi.org/10.1038/emm.2015.33> PMID:26045254
16. Pérez-Juste G, García-Silva S, Aranda A. An element in the region responsible for premature termination of transcription mediates repression of c-myc gene expression by thyroid hormone in neuroblastoma cells. *J Biol Chem*. 2000; 275:1307–14. <https://doi.org/10.1074/jbc.275.2.1307> PMID:10625678
17. Bell AC, West AG, Felsenfeld G. The protein CTCF is required for the enhancer blocking activity of vertebrate insulators. *Cell*. 1999; 98:387–96. [https://doi.org/10.1016/s0092-8674\(00\)81967-4](https://doi.org/10.1016/s0092-8674(00)81967-4) PMID:10458613
18. Oh S, Oh C, Yoo KH. Functional roles of CTCF in breast cancer. *BMB Rep*. 2017; 50:445–53. <https://doi.org/10.5483/bmbrep.2017.50.9.108> PMID:28648147
19. Holwerda SJ, de Laat W. CTCF: the protein, the binding partners, the binding sites and their chromatin loops. *Philos Trans R Soc Lond B Biol Sci*. 2013; 368:20120369. <https://doi.org/10.1098/rstb.2012.0369> PMID:23650640
20. Yu X, Liu Q, He J, Huang Y, Jiang L, Xie X, Liu J, Chen L, Wei L, Qin Y. Vigilin interacts with CTCF and is involved in the maintenance of imprinting of IGF2 through a novel RNA-mediated mechanism. *Int J Biol Macromol*. 2018; 108:515–22. <https://doi.org/10.1016/j.ijbiomac.2017.11.109> PMID:29157910
21. Chao W, Huynh KD, Spencer RJ, Davidow LS, Lee JT. CTCF, a candidate trans-acting factor for x-inactivation choice. *Science*. 2002; 295:345–47. <https://doi.org/10.1126/science.1065982> PMID:11743158
22. Zhang B, Zhang Y, Zou X, Chan AW, Zhang R, Lee TK, Liu H, Lau EY, Ho NP, Lai PB, Cheung YS, To KF, Wong HK, et al. The CCCTC-binding factor (CTCF)-forkhead box protein M1 axis regulates tumour growth and metastasis in hepatocellular carcinoma. *J Pathol*. 2017; 243:418–30. <https://doi.org/10.1002/path.4976> PMID:28862757
23. Guo Y, Perez AA, Hazelett DJ, Coetzee GA, Rhie SK, Farnham PJ. CRISPR-mediated deletion of prostate cancer risk-associated CTCF loop anchors identifies repressive chromatin loops. *Genome Biol*. 2018; 19:160. <https://doi.org/10.1186/s13059-018-1531-0> PMID:30296942
24. Delgado MD, Chernukhin IV, Bigas A, Klenova EM, León J. Differential expression and phosphorylation of CTCF, a c-myc transcriptional regulator, during differentiation of human myeloid cells. *FEBS Lett*. 1999; 444:5–10. [https://doi.org/10.1016/s0014-5793\(99\)00013-7](https://doi.org/10.1016/s0014-5793(99)00013-7) PMID:10037138
25. Klenova EM, Fagerlie S, Filippova GN, Kretzner L, Goodwin GH, Loring G, Neiman PE, Lobanenkov VV. Characterization of the chicken CTCF genomic locus, and initial study of the cell cycle-regulated promoter of the gene. *J Biol Chem*. 1998; 273:26571–79. <https://doi.org/10.1074/jbc.273.41.26571> PMID:9756895

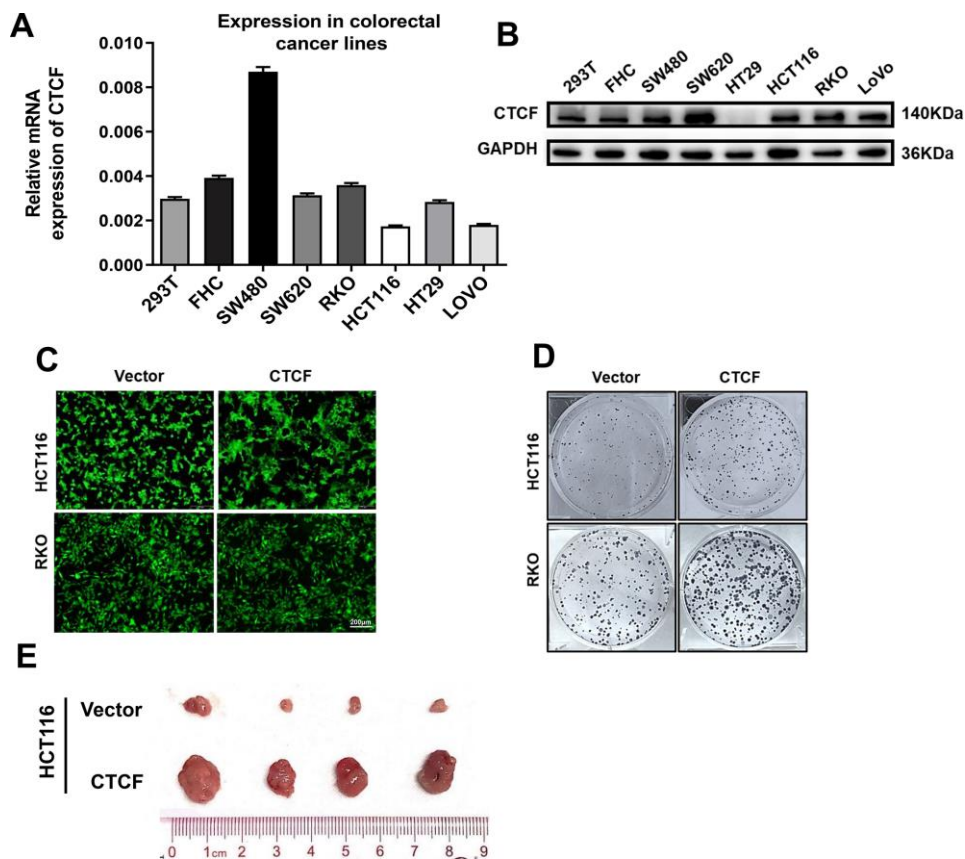
26. Yan H, Tang G, Wang H, Hao L, He T, Sun X, Ting AH, Deng A, Sun S. DNA methylation reactivates GAD1 expression in cancer by preventing CTCF-mediated polycomb repressive complex 2 recruitment. *Oncogene*. 2016; 35:3995–4008. <https://doi.org/10.1038/onc.2015.423> PMID:26549033
27. Lee JY, Mustafa M, Kim CY, Kim MH. Depletion of CTCF in breast cancer cells selectively induces cancer cell death via p53. *J Cancer*. 2017; 8:2124–31. <https://doi.org/10.7150/jca.18818> PMID:28819414
28. Batlle-López A, Cortiguera MG, Rosa-Garrido M, Blanco R, del Cerro E, Torrano V, Wagner SD, Delgado MD. Novel CTCF binding at a site in exon1A of BCL6 is associated with active histone marks and a transcriptionally active locus. *Oncogene*. 2015; 34:246–56. <https://doi.org/10.1038/onc.2013.535> PMID:24362533
29. Chang JW, Hsu HS, Ni HJ, Chuang CT, Hsiung CH, Huang TH, Wang YC. Distinct epigenetic domains separated by a CTCF bound insulator between the tandem genes, BLU and RASSF1A. *PLoS One*. 2010; 5:e12847. <https://doi.org/10.1371/journal.pone.0012847> PMID:20877461
30. Witcher M, Emerson BM. Epigenetic silencing of the p16(INK4a) tumor suppressor is associated with loss of CTCF binding and a chromatin boundary. *Mol Cell*. 2009; 34:271–84. <https://doi.org/10.1016/j.molcel.2009.04.001> PMID:19450526
31. Zhao L, Yang Y, Yin S, Yang T, Luo J, Xie R, Long H, Jiang L, Zhu B. CTCF promotes epithelial ovarian cancer metastasis by broadly controlling the expression of metastasis-associated genes. *Oncotarget*. 2017; 8:62217–30. <https://doi.org/10.18632/oncotarget.19216> PMID:28977939
32. Giannakis M, Mu XJ, Shukla SA, Qian ZR, Cohen O, Nishihara R, Bahl S, Cao Y, Amin-Mansour A, Yamauchi M, Sukawa Y, Stewart C, Rosenberg M, et al. Genomic correlates of immune-cell infiltrates in colorectal carcinoma. *Cell Rep*. 2016; 17:1206. <https://doi.org/10.1016/j.celrep.2016.10.009> PMID:27760322
33. Tang Z, Li C, Kang B, Gao G, Li C, Zhang Z. GEPIA: a web server for cancer and normal gene expression profiling and interactive analyses. *Nucleic Acids Res*. 2017; 45:W98–102. <https://doi.org/10.1093/nar/gkx247> PMID:28407145
34. Hsu HH, Chen MC, Baskaran R, Lin YM, Day CH, Lin YJ, Tu CC, Vijaya Padma V, Kuo WW, Huang CY. Oxaliplatin resistance in colorectal cancer cells is mediated via activation of ABCG2 to alleviate ER stress induced apoptosis. *J Cell Physiol*. 2018; 233:5458–67. <https://doi.org/10.1002/jcp.26406> PMID:29247488
35. Giroux-Leprieur E, Costantini A, Ding VW, He B. Hedgehog signaling in lung cancer: from oncogenesis to cancer treatment resistance. *Int J Mol Sci*. 2018; 19:2835. <https://doi.org/10.3390/ijms19092835> PMID:30235830
36. Huang FT, Zhuan-Sun YX, Zhuang YY, Wei SL, Tang J, Chen WB, Zhang SN. Inhibition of hedgehog signaling depresses self-renewal of pancreatic cancer stem cells and reverses chemoresistance. *Int J Oncol*. 2012; 41:1707–14. <https://doi.org/10.3892/ijo.2012.1597> PMID:22923052
37. Amantini C, Morelli MB, Nabissi M, Cardinali C, Santoni M, Gismondi A, Santoni G. Capsaicin triggers autophagic cell survival which drives epithelial mesenchymal transition and chemoresistance in bladder cancer cells in an hedgehog-dependent manner. *Oncotarget*. 2016; 7:50180–94. <https://doi.org/10.18632/oncotarget.10326> PMID:27367032
38. Allegra C, Sargent DJ. Adjuvant therapy for colon cancer—the pace quickens. *N Engl J Med*. 2005; 352:2746–48. <https://doi.org/10.1056/NEJMe058117> PMID:15987925
39. Cremolini C, Loupakis F, Antoniotti C, Lupi C, Sensi E, Lonardi S, Mezi S, Tomasello G, Ronzoni M, Zaniboni A, Tonini G, Carlomagno C, Allegrini G, et al. FOLFOXIRI plus bevacizumab versus FOLFIRI plus bevacizumab as first-line treatment of patients with metastatic colorectal cancer: updated overall survival and molecular subgroup analyses of the open-label, phase 3 TRIBE study. *Lancet Oncol*. 2015; 16:1306–15. [https://doi.org/10.1016/S1470-2045\(15\)00122-9](https://doi.org/10.1016/S1470-2045(15)00122-9) PMID:26338525
40. Limagne E, Euvrard R, Thibaudin M, Rébé C, Derangère V, Chevriaux A, Boidot R, Végran F, Bonnefoy N, Vincent J, Bengrine-Lefevre L, Ladoire S, Delmas D, et al. Accumulation of MDSC and Th17 cells in patients with metastatic colorectal cancer predicts the efficacy of a FOLFOX-bevacizumab drug treatment regimen. *Cancer Res*. 2016; 76:5241–52. <https://doi.org/10.1158/0008-5472.CAN-15-3164> PMID:27496709
41. Guo Y, Xiong BH, Zhang T, Cheng Y, Ma L. XELOX vs. Folfox in metastatic colorectal cancer: an updated meta-analysis. *Cancer Invest*. 2016; 34:94–104. <https://doi.org/10.3109/07357907.2015.1104689>

PMID:[26864862](#)

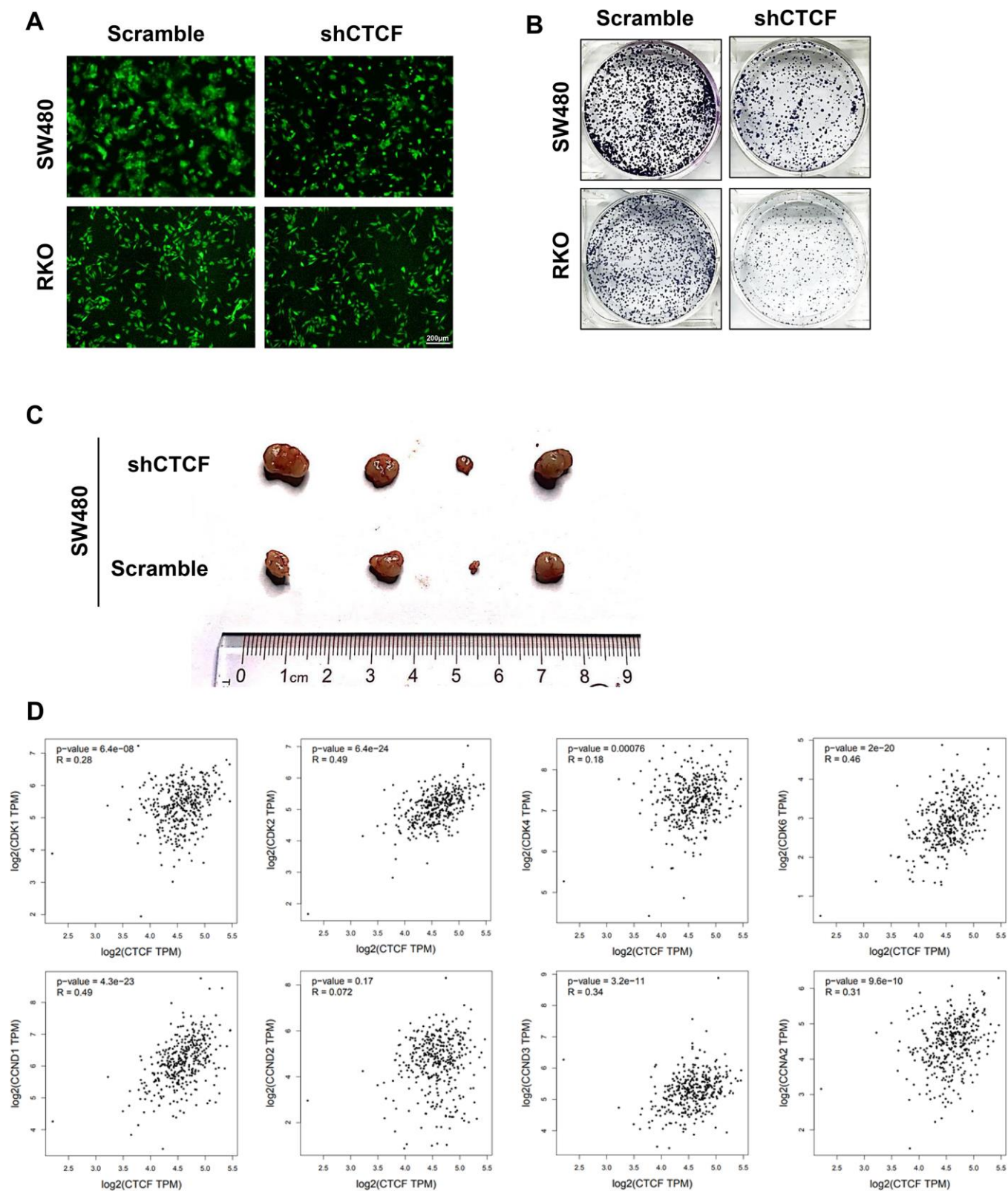
42. Toyoda Y, Takada T, Suzuki H. Inhibitors of human ABCG2: from technical background to recent updates with clinical implications. *Front Pharmacol.* 2019; 10:208.
<https://doi.org/10.3389/fphar.2019.00208>
PMID:[30890942](#)
43. Cai D, Yu J, Qiu J, He B, Chen Z, Yan M, Liu Q. Dynamic changes of sonic hedgehog signaling pathway in gastric mucosa of rats with MNNG-induced gastric precancerous lesions. *J Cell Physiol.* 2019; 234:10827–34.
<https://doi.org/10.1002/jcp.27908> PMID:[30537251](#)
44. Salaritabar A, Berindan-Neagoe I, Darvish B, Hadjiakhoondi F, Manayi A, Devi KP, Barreca D, Orhan IE, Süntar I, Farooqi AA, Gulei D, Nabavi SF, Sureda A, et al. Targeting hedgehog signaling pathway: paving the road for cancer therapy. *Pharmacol Res.* 2019; 141:466–80.
<https://doi.org/10.1016/j.phrs.2019.01.014>
PMID:[30639373](#)
45. Giroux Leprieur E, Vieira T, Antoine M, Rozensztajn N, Rabbe N, Ruppert AM, Lavole A, Cadranel J, Wislez M. Sonic hedgehog pathway activation is associated with resistance to platinum-based chemotherapy in advanced non-small-cell lung carcinoma. *Clin Lung Cancer.* 2016; 17:301–08.
<https://doi.org/10.1016/j.clcl.2015.12.007>
PMID:[26762562](#)
46. Singh RR, Kunkalla K, Qu C, Schlette E, Neelapu SS, Samaniego F, Vega F. ABCG2 is a direct transcriptional target of hedgehog signaling and involved in stroma-induced drug tolerance in diffuse large b-cell lymphoma. *Oncogene.* 2011; 30:4874–86.
<https://doi.org/10.1038/onc.2011.195> PMID:[21625222](#)
47. Xu F, Ye ML, Zhang YP, Li WJ, Li MT, Wang HZ, Qiu X, Xu Y, Yin JW, Hu Q, Wei WH, Chang Y, Liu L, Zhao Q. MicroRNA-375-3p enhances chemosensitivity to 5-fluorouracil by targeting thymidylate synthase in colorectal cancer. *Cancer Sci.* 2020; 111:1528–41.
<https://doi.org/10.1111/cas.14356>
PMID:[32073706](#)
48. Liang Y, Hou L, Li L, Li L, Zhu L, Wang Y, Huang X, Hou Y, Zhu D, Zou H, Gu Y, Weng X, Wang Y, et al. Dichloroacetate restores colorectal cancer chemosensitivity through the p53/miR-149-3p/PDK2-mediated glucose metabolic pathway. *Oncogene.* 2020; 39:469–85.
<https://doi.org/10.1038/s41388-019-1035-8>
PMID:[31597953](#)
49. Joerger AC, Fersht AR. The p53 pathway: origins, inactivation in cancer, and emerging therapeutic approaches. *Annu Rev Biochem.* 2016; 85:375–404.
<https://doi.org/10.1146/annurev-biochem-060815-014710> PMID:[27145840](#)
50. Chung JH, Larsen AR, Chen E, Bunz F. A PTCH1 homolog transcriptionally activated by p53 suppresses hedgehog signaling. *J Biol Chem.* 2014; 289:33020–31.
<https://doi.org/10.1074/jbc.M114.597203>
PMID:[25296753](#)
51. Li Q, Lai Q, He C, Fang Y, Yan Q, Zhang Y, Wang X, Gu C, Wang Y, Ye L, Han L, Lin X, Chen J, et al. RUNX1 promotes tumour metastasis by activating the Wnt/ β -catenin signalling pathway and EMT in colorectal cancer. *J Exp Clin Cancer Res.* 2019; 38:334.
<https://doi.org/10.1186/s13046-019-1330-9>
PMID:[31370857](#)
52. Wang X, Lan Z, He J, Lai Q, Yao X, Li Q, Liu Y, Lai H, Gu C, Yan Q, Fang Y, Zhang Y, Li A, Liu S. LncRNA SNHG6 promotes chemoresistance through ULK1-induced autophagy by sponging miR-26a-5p in colorectal cancer cells. *Cancer Cell Int.* 2019; 19:234.
<https://doi.org/10.1186/s12935-019-0951-6>
PMID:[31516391](#)

SUPPLEMENTARY MATERIALS

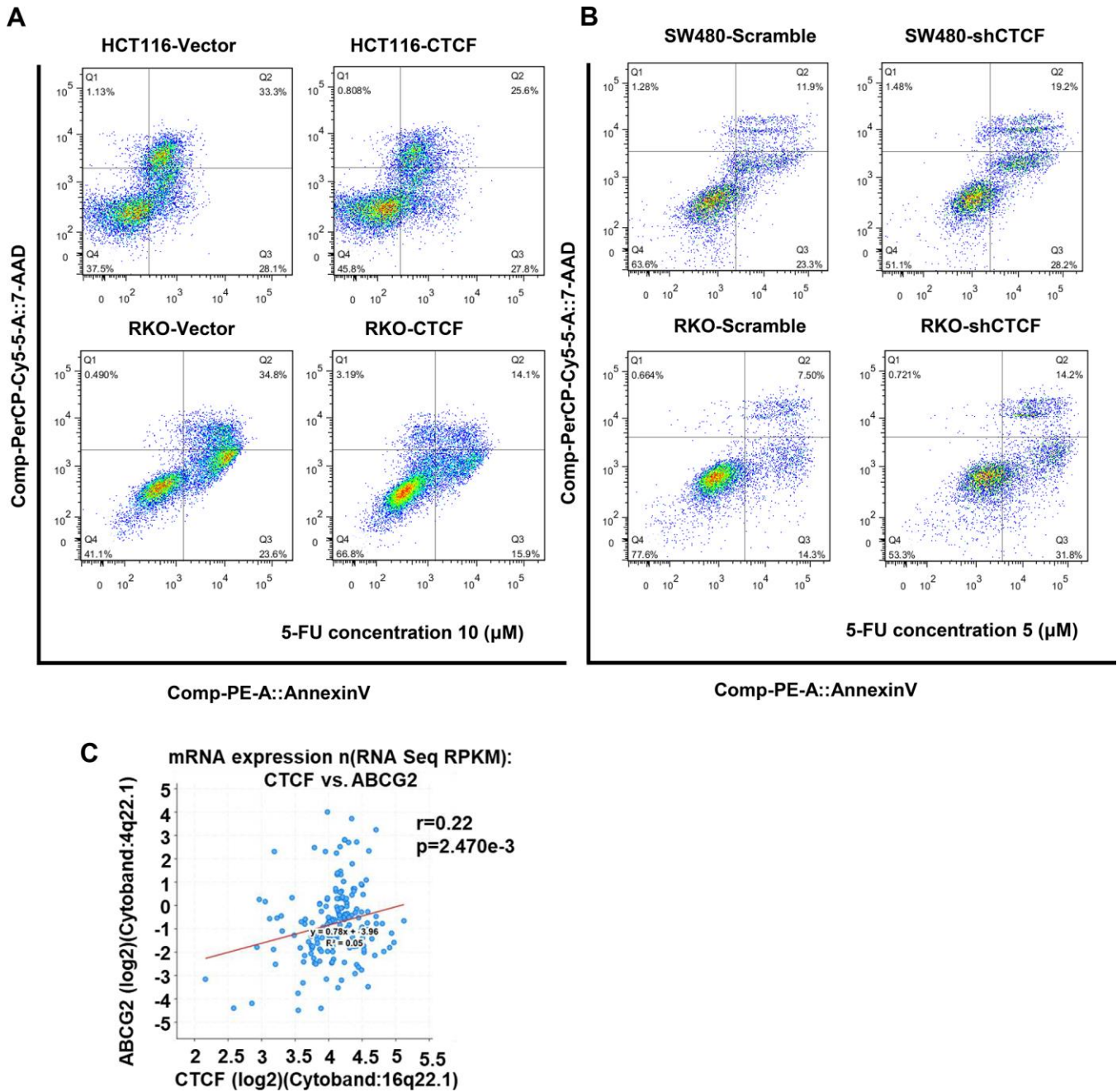
Supplementary Figures



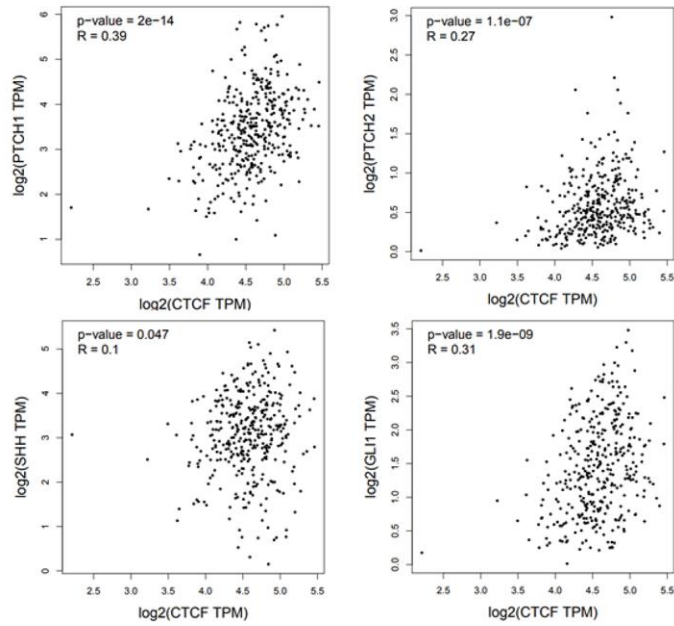
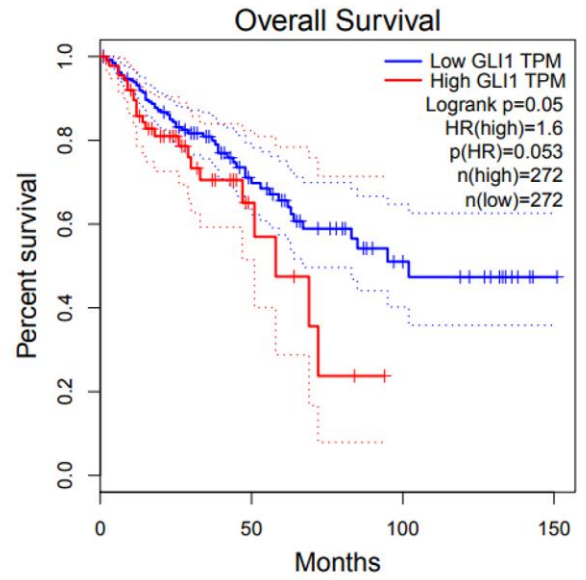
Supplementary Figure 1. Overexpression of CTCF enhances human CRC cells proliferative capacity. (A) mRNA level of CTCF in human embryonic kidney cell line (293T), human normal colon epithelial cell line (FHC) and six CRC cell lines. (B) Western blot analysis of human embryonic kidney cell line (293T), human normal colon epithelial cell line (FHC) and six CRC cell lines. The above data are presented as mean \pm SEM. (C) Fluorescence assessment of the green fluorescent protein (GFP). Vector represents lentivirus-mediated control groups. CTCF represents lentivirus-mediated CTCF overexpressing groups. (D) The representative images of colony formation assay from different experimental groups are shown. (E) Corresponding cells were respectively injected subcutaneously into the right and left back hips of nude mice (n = 4). Representative images of the tumors are shown. * P<0.05, **P<0.01, and ***P<0.001.



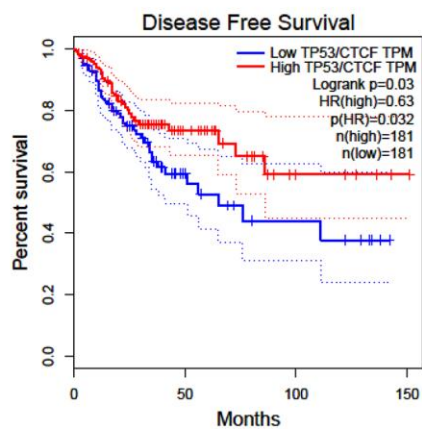
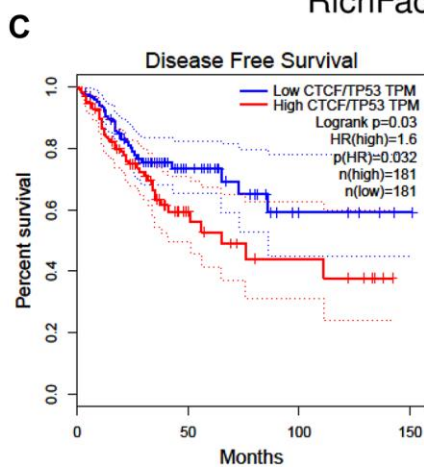
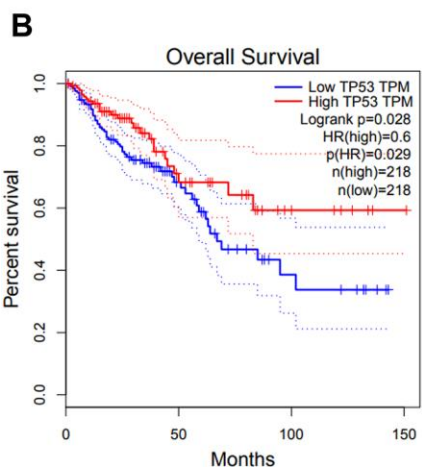
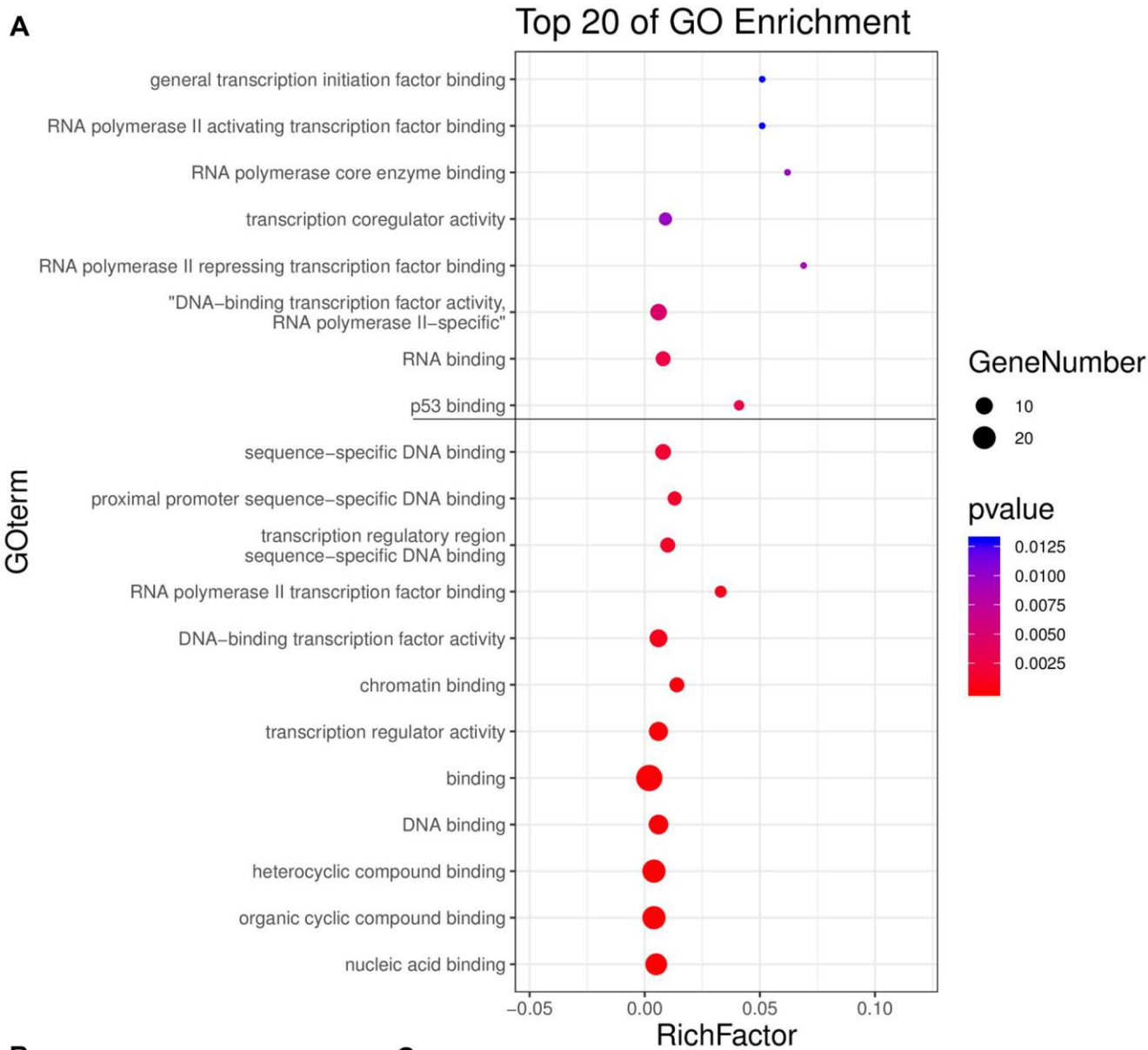
Supplementary Figure 2. Knockdown of CTCF inhibits human CRC cells proliferation. (A) Fluorescence assessment of the green fluorescent protein (GFP). Scramble represents lentivirus-mediated control groups. shCTCF represents lentivirus-mediated CTCF silencing groups. (B) The representative images of colony formation assays from different experimental groups are shown. (C) Corresponding cells were respectively injected subcutaneously into the right and left back hips of nude mice (n = 4). Representative images of the tumors are shown. (D) CTCF expression was positively correlated with the expression of CDKs and Cyclins in GEPIA (<http://gepia.cancer-pku.cn/>).



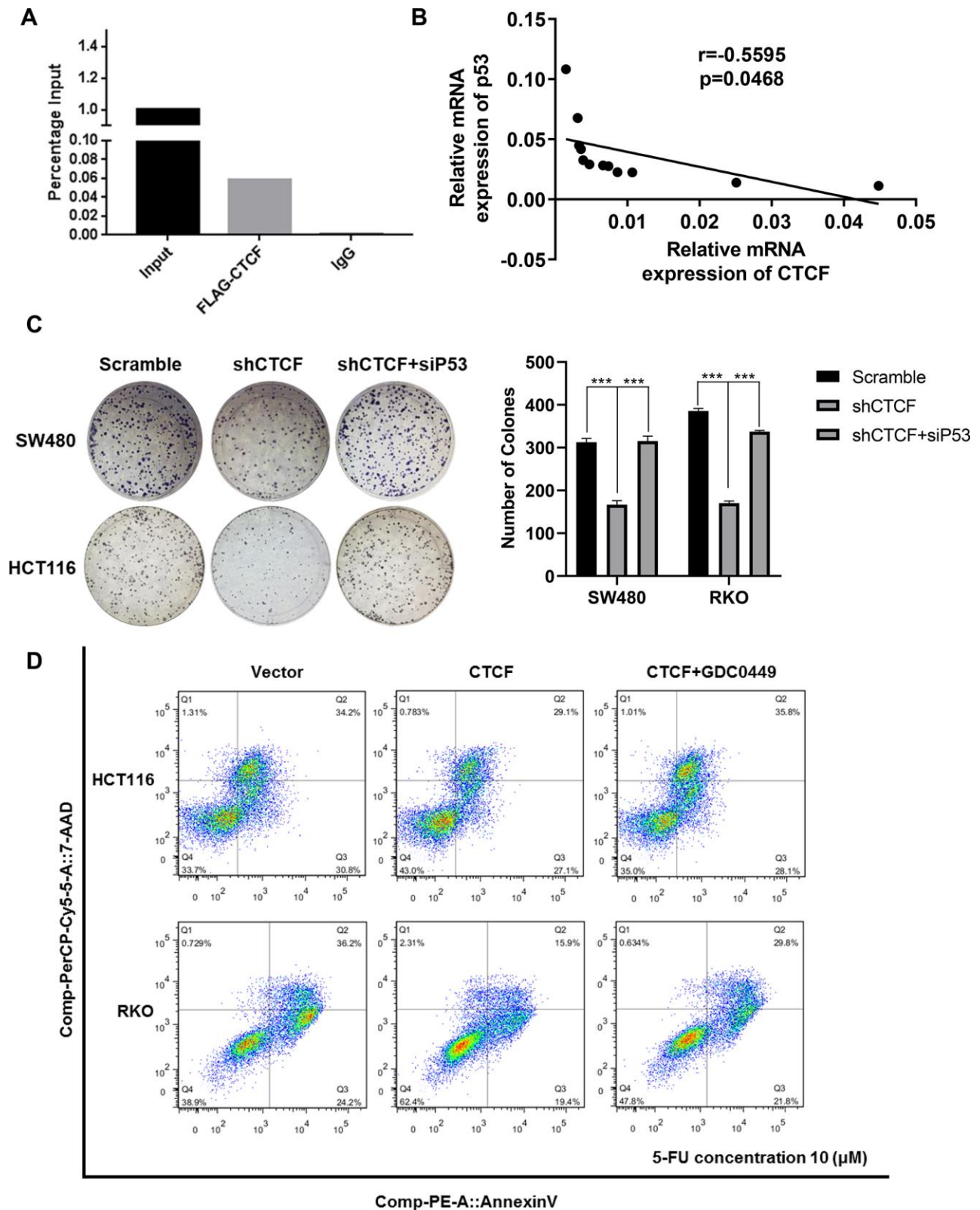
Supplementary Figure 3. CTCF causes CRC cells to be insensitive to 5-FU-based chemoresistance. (A, B) The representative images of apoptotic assays from different experimental groups are shown. Scramble and shCTCF cell lines were treated with 5-FU with a 5 μ M concentration, and the other cell lines were treated with 5-FU with a 10 μ M concentration. (C) Positive correlation between CTCF expression and ABCG2 by spearman correlation analysis in cBioPortal (<http://www.cbioportal.org/>).

A**B**

Supplementary Figure 4. CTCF activates Hedgehog signaling pathway. (A) Positive correlation between CTCF expression and the key molecules of Hedgehog signaling pathway by spearman correlation analysis in GEPIA (<http://gepia.cancer-pku.cn/>). (B) Kaplan-Meier survival analysis revealed that CRC patients in the GLI1 high expression group have shorter survival time in GEPIA.



Supplementary Figure 5. CTCF might regulate P53 in CRC. (A) GO-molecular function enrichment analysis of the top 30 similar genes of CTCF in GEPIA is shown. (B) Kaplan-Meier survival analysis revealed that CRC patients in the TP53 high expression group have good prognosis in GEPIA. (C) Kaplan-Meier survival analysis showed that the ratio of CTCF/TP53 is positively related to disease free survival time.



Supplementary Figure 6. CTCF facilitates CRC progression via P53-Hedgehog axis. (A) ChIP-qPCR results for CTCF on the CBS in HCT116 cells. (B) Spearman correlation analysis between relative CTCF and P53 mRNA expression in 13 fresh human CRC specimens. (C) Cell proliferative capacity was tested by colony formation assays and the representative images of colony formation assays from different experimental groups are shown. (D) The representative images of apoptotic assays from different experimental groups with or without administration of GDC-0449 are shown. The above data are presented as mean \pm SEM. * $P < 0.05$, ** $P < 0.01$, and *** $P < 0.001$.

Supplementary Table

Supplementary Table 1. Primer sequences used for real-time PCR or CHIP-PCR (5' to 3').

Gene	Forward primer	Reverse primer
GAPDH	CGAGCCACATCGCTCAGACA	GTGGTGAAGACGCCAGTGGA
CTCF	CCCAAACAGAACCAGCCAAC	TCCTCTCCTCTCCCTCTGC
ABCG2	CTCTTCTTCCTGACGACCAACCA	ATGACACTCTGTAGTATCCGCTGAT
TP53	CAGCACATGACGGAGGTTGT	TCATCCAAATACTCCACACGC
CTCF-CBS	CATTGTTGTATTCCTGAGTGCC	GAGTCCCGCGGTAAT TCTT